

PRELIMINARY TESTING OF A TWO-CYLINDER
TWO-STROKE LEAN BURN ENGINE OF THE
INTER-CYLINDER CONNECTING PORT TYPE

Peter Robert Csatory

A project report submitted to the Faculty of Engineering, University of
the Witwatersrand, Johannesburg, in partial fulfillment of the requirements
for the degree of Master of Science in Engineering

Johannesburg, 1985

DECLARATION

I declare that this project report is my own work. It is being submitted in part fulfilment for the Degree of Master of Science in Engineering in the University of the Witwatersrand, Johannesburg. It has not been submitted before for any degree or examination in any other University.

Pontory

15th day of November 1985

PREFACE

The University offers several routes to the degree of MSc(Eng). The one chosen by the author was by advanced coursework and a four month full time equivalent research project. This report submitted reflects the latter component of the degree requirements.

Such project reports are to take the form primarily of a paper for publication and, where appropriate, supported by appendices or other documents. The paper is thus intended to stand by itself, with separate abstract, figures, references and acknowledgments. The appendices are provided largely for internal use by future researchers at the University requiring a more complete record of the project.

The format of this paper is in keeping with that of publications of the Society of Automotive Engineers (SAE). The intended readership are engineers who are not necessarily familiar with the principles of lean-burn operation of internal combustion engines.

ABSTRACT

Lean burn combustion has long been recognised as a means of increasing engine efficiency and reducing pollutant emissions. In this study, the commissioning and testing of a particular form of such an engine is reported. The engine is a two-stroke, two-cylinder machine, the pistons of which move in unison. An inter-cylinder connecting port was intended to allow very lean mixtures to be reliably ignited in one cylinder, by a flame torch travelling through this port from the other approximately stoichiometrically charged cylinder. Lack of primary balance was found to lead to excessive vibration at speeds over 2000 rpm. The tests indicate that the design of the combustion chambers (at present of the disc type) and of the inter-cylinder connecting port are unsatisfactory. Recommendations on the redesign of the engine (or the possible replacement of the engine with a better balanced model) and of the test facility in the interests of improved system performance and reliability are provided. The material is presented briefly in the form of a paper for publication and in a number of supportive appendices.

ACKNOWLEDGMENTS

The author offers his thanks to the following:

- * Mr R M Amm for making available an early version of the lean burn engine which was the subject of this study
- * The Anglo American Corporation of South Africa for financial contribution to this project
- * The Council for Scientific and Industrial Research for providing a bursary for postgraduate study
- * Professor C J Railis, for his technical guidance and enthusiasm during testing
- * Dr R H Jawurek, for his guidance and assistance in the editing and presentation of this report
- * Mr N W Lane for giving generously of his time and expertise in data acquisition and processing
- * The entire technical staff of the Mechanical Engineering Laboratory for their many and varied contributions to the construction of the test rig
- * Mrs H Leath for her patient and accurate typing of the manuscript

CONTENTS

	Page
DECLARATION	1
PREFACE	1f
ABSTRACT	11f
ACKNOWLEDGMENTS	1v
CONTENTS	v
LIST OF FIGURES	v1f
LIST OF TABLES	x1

PAPER FOR PUBLICATION: Preliminary Testing of a Two-Cylinder Two-Stroke Lean Burn engine of the Inter-Cylinder Connecting Port Type 1

APPENDIX A - LEAN BURN ENGINES: A GENERAL INTRODUCTION

A.1	Definition of Lean Burn Engines	A1
A.2	The Need for Lean Burn Engines	A2
A.3	The Formation of Pollutants	A3
A.4	Techniques of Achieving Lean Burn/Stratified Charge Operation	A4
A.5	Introduction of the Research Engine of this Study	A7
A.6	Classifying the Research Engine	A9

APPENDIX B - SURVEY OF LITERATURE

B.1	Introduction to Lean Burn Engines	B3
B.2	Engine Designs Related to the Research Engine	B5
B.2.1	The Honda Compound Vortex Controlled Combustion (CVCC) engine	B5
B.2.2	The Porsche stratified charge (SC) engine	B7
B.2.3	The staged combustion compound engine (SCCE)	B9
B.2.4	Two-stroke cycle lean burn designs	B11
B.2.5	The May-Fireball head	B16
B.2.6	The Cranfield-Kushul (C-K) engine	B19
B.3	Specific Areas of Study	B22
B.3.1	Ignition systems	B22

B.3.2	Orifice and pre-combustion chamber size and shape	B26
B.3.3	External devices	B31
B.3.4	Combustion chamber size and shape	B31
B.3.5	Fully open air throttling	B31
B.4	Miscellaneous	B32

APPENDIX C - DESCRIPTION OF THE RESEARCH ENGINE

C.1	Basic Engine Dimensions	C1
C.2	Engine Modifications by Past Researchers	C5
C.3	Further Modifications During the Present Study	C9

APPENDIX D - INSTRUMENTATION

D.1	Test System Parameters	D1
D.1.1	System inputs	D2
D.1.2	System outputs	D2
D2	Specification and Calibration of Instruments	D4
D.2.1	Combustion chamber pressures	D4
D.2.2	Fuel consumption	D5
D.2.3	Torque	D12
D.2.4	Mass flow rate of air	D14
D.2.5	Inlet air temperature	D15
D.2.6	Exhaust pressure	D16
D.2.7	Transfer port differential pressure	D16
D.3	Data Processing	D16
D.3.1	Computerization requirements	D17
D.3.2	Incorporation into instrumentation system	D19
D.3.3	Computer program	D20

APPENDIX E - RESULTS

E.1	Intended Test Procedure	E1
E.2	Results Obtained	E2

APPENDIX F - REFERENCES

LIST OF FIGURES

Figure	Page
1 Example of lean burn operation in engine with one prechamber	4
2 Schematic of combustion chambers modified for lean burn operation (not to scale)	6
3 Research engine: mode of operation	7
4 Cross section of Honda CVCC engine (after Date et al)	8
5 Cranfield-Kushul engine: mode of operation (after Beale and Hodgetts)	10
6 Pressure versus time trace: mixture cylinder	16
7 Pressure versus time trace: mixture and air cylinders	16
8 Schematic of original Yamaha 55EM cylinder head	18
A1 Pollutant formation within an engine	A3
A2 Example of lean burn operation in engine with one prechamber	A5
A3 Classification system for reciprocating IC engines	A6
A4 Mode of operation of the research engine	A8
B1 Classification of research engine and related designs	B2
B2 Trend in compression ratios of US cars	B4
B3 Comparison of turbulent flow manifold with standard intake manifold	B5
B4 Sectional view of Honda CVCC cylinder	B6
B5 Exhaust gas emissions of CVCC engine and a conventional engine at idling (Isfc = 410 g/PS-hr)	B7
B6 Cross-section of Porsche SC cylinder	B8
B7 Exhaust emissions of Porsche SC engine compared with conventional engine	B9
B8 One-staged combustion compound engine	B10
B9 The effect of trapping efficiency on cycle thermal efficiency	B12
B10 YCCP process; Cylinder head showing residue gas	B13
B11 MULS engine scavenging	B15

	Page
B12 The May Fireball combustion chamber	B16
B13 Cranfield-Kushul engine operating phases	B19
B14 Variation of the brake specific fuel consumption with brake load	B21
B15 Variation of NO emissions with indicated load	B21
B16 Variation of CO emissions with indicated load	B21
B17 Variation of HC emissions with indicated load	B21
B18 Effect of gap width and centre electrode diameter on lean limit	B23
B19 Improvement of lean limit by widening gap width	B23
B20 Effect of gap width and spark timing on the lean limit	B23
B21 Effect of spark plug gap projection on lean limit	B24
B22 Effect of spark energy on lean limits	B24
B23 Combustion chamber design of single cylinder engine with dual ignition	B25
B24 Cross section of CFR engine	B27
B25 Effect of stratification and overall equivalence ratio on fuel consumption	B28
B26 Branched conduit type of combustion chamber	B29
B27 Anti-knock quality of stratified charge engines	B29
B28 Cross section of combustion chamber	B30
B29 Effects of orifice dimensions	B30
C1 Production Yamaha 55 BM engine	C2
C2 Cylinder port location and dimensions	C3
C3 Piston depth vs crank angle	C4
C4 Port timing on research engine	C5
C5 Cylinder head and water cooling jacket	C7
C6 Cylinder head assembly	C7
C7 Starter motor assembly	C10
C8 Fuel flow throttling device	C11
C9 Needle housing	C12
C10 Fuel needle	C13
C11 Main fuel jet	C14

	Page
C12 Air cylinder lubricant reserve	C15
D1 Logic diagram of engine inputs and outputs	D1
D2 Exhaust pressure datum	D4
D3 Water cooled transducer housing - disassembled and assembled into cylinder head with transducer	D4
D4 Glass bowl fuel flow meter	D6
D5 Pierburg fuel flow meters in fuel supply line	D8
D6 Calibration : Pierburg 3749 fuel flow meter	D9
D7 Calibration : Pierburg 2542 fuel flow meter	D11
D8 Dynamometer calibration	D13
D9 Operation of TDC trigger circuit	D18
D10 Voltage comparator circuit	D19
D11 Flowchart of computer program	D21
E1 Intended power-speed curves for one air throttle setting	E1
E2 Pressure trace - mixture cylinder: Test 1	E3
E3 Pressure trace - air cylinder: Test 1	E4
E4 Pressure trace - differential across cylinders: Test 1	E5
E5 Spark ignition timing: Test 1	E6
E6 Pressure trace - mixture cylinder: Test 09108501	E8
E7 Pressure trace - air cylinder: Test 09108501	E9
E8 Pressure trace - both cylinders: Test 09108501	E10
E9 Pressure trace - differential across cylinders: Test 09108501	E11
E10 Spark ignition timing: Test 09108501	E12
E11 Pressure trace - mixture cylinder: Test 09108502	E14
E12 Pressure trace - air cylinder: Test 09108502	E15
E13 Pressure trace - both cylinders: Test 09108502	E16
E14 Pressure trace - differential across cylinders: Test 09108502	E17
E15 Spark ignition timing: Test 09108502	E18
E16 Pressure trace - mixture cylinder: Test 09108503	E19
E17 Pressure trace - air cylinder: Test 09108503	E20
E18 Pressure trace - both cylinders: Test 09108503	E21
E19 Pressure trace - differential across cylinders: Test 09108503	E22

X

	Page
E20 Spark ignition timing - Test 09108503	E23
E21 Pressure trace - mixture cylinder: Test 09108504	E24
E22 Pressure trace - air cylinder: Test 09108504	E25
E23 Pressure trace - both cylinders: Test 09108504	E26
E24 Pressure trace - differential across cylinders: Test 09108504	E27
E25 Spark ignition timing: Test 09108504	E28
E26 Required fuel flow for AFR = 12,5:1	E30
E27 Pressure trace - mixture cylinder: Test 10108501	E33
E28 Pressure trace - air cylinder: Test 10108501	E34
E29 Pressure trace - both cylinders: Test 10108501	E35
E30 Pressure trace - differential across cylinders: Test 10108501	E36
E31 Spark ignition timing: Test 10108501	E37

LIST OF TABLES

Table	Page
B1 Car data: May Fireball vs standard engine and Honda CVCC	B18
C1 Piston depth (below cylinder sleeve) vs crank angle	C3
D1 Calibration of glass bowl fuel flow meters	D7
D2 Pierburg 3749 fuel flow meter calibration - mixture cylinder	D8
D3 Pierburg 2542 fuel flow meter calibration - air cylinder	D10
D4 Dynamometer calibration	D12
E1 Test results, code 09108501 - 09108503	E7

Preliminary Testing of a Two-Cylinder Two-Stroke Lean Burn Engine of the Inter-Cylinder Connecting Port Type

Peter R Csatary

School of Mechanical Engineering
University of the Witwatersrand

ABSTRACT

Lean burn combustion has long been recognised as a means of increasing engine efficiency and reducing pollutant emissions. In this paper, the commissioning and testing of a particular form of such an engine is reported. The engine is a two-stroke, two-cylinder machine, the pistons of which move in unison. An inter-cylinder connecting port was intended to allow lean mixtures to be reliably ignited in one cylinder, by a flame torch travelling through this port from the other approximately stoichiometrically charged cylinder. Lack of primary balance was found to lead to excessive vibration at speeds over 2000 rpm. The tests indicate that the design of the combustion chambers (at present of the disc type) and of the inter-cylinder connecting port are *unsatisfactory*. Recommendations on the redesign of the engine (or the possible replacement of the engine with a better balanced model) and of the test facility in the interests of improved system performance and reliability are presented.

INTRODUCTION

Both lean burn (LB) and stratified charge (SC) reciprocating internal combustion (IC) engines operate with an overall air-fuel ratio (AFR) considerably higher (weaker) than that of conventional engines (1). Numerous techniques are used to allow operation beyond the lean misfire limit of conventional engines, and some of these are discussed in the following section.

The two major motivators for finding a replacement for the conventional spark ignition (SI) engine are the need to decrease the emissions of hydrocarbons (HC), carbon monoxide (CO) and oxides of nitrogen (NO_x), and to improve fuel economy.

Further, the above improvements are required to be achieved without sacrificing engine performance. A great step in the reduction of toxic emission of pollutants would be the use of unleaded fuel. This usually implies that the compression ratio (CR) has to be lowered, resulting in reduced performance and greater fuel consumption as the lean misfire limit is decreased to a richer mixture.

An additional advantage of LB operation is the improvement in the thermal efficiency of the engine cycle. Thermal efficiency is directly related to the CR of the engine, which can always be raised when LB techniques are used. A further advantage is that most production LB engines do not require catalytic converters to meet emission specification laws in the United States at present, and in European countries in the near future.

Lean burn research has also provided a revival of interest in the two-stroke cycle engine. At present, two-stroke engines are used largely where ultra high performance is required (motorcycle racing) or where cheapness and operation over a limited speed range are sought (generator motors, lawnmowers). The former use dictates large cylinder port areas and results in high emission of pollutants at part load, high fuel consumption and erratic operation at low load. By using LB techniques

these disadvantages may be overcome, whilst retaining the advantages of simple construction and high performance.

Production examples of LB engines already exist. The better known automobile models are the Honda CVCC, the Ford PROCO and the Jaguar XJS. Numerous research and development programs aimed at LB designs having improved emission and performance characteristics, and reduced fuel consumption are in progress world-wide. The project here reported forms a small part of this overall effort.

The specific objectives of the project were to complete the instrumentation and the preliminary testing of the lean burn research engine which is under study in our laboratory.

LEAN BURN TECHNIQUES

The terms 'lean burn' and 'stratified charge' differ in significance, although they have been used interchangeably on occasion. In some engine designs both techniques are applied to achieve the common objective of low emissions from lean overall mixtures.

Lean burn engines generally utilize a finite number (between one and three) mixtures of different AFR'S. In a typical lean burn engine, rich mixture is ignited in a pre-combustion chamber and the flame front subsequently propagates into the main chamber (via an orifice) which contains a weaker mixture (Figure 1). An LB engine using only one homogeneous AFR would need to generate very high mixture turbulence to guarantee reliable ignition.

Stratified charge engines, on the other hand, create a continuous gradient of varying AFR in all three dimensions, based on density differences. No physical boundary exists between these layers, and the process is often improved by careful design to achieve swirl of the incoming mixture.

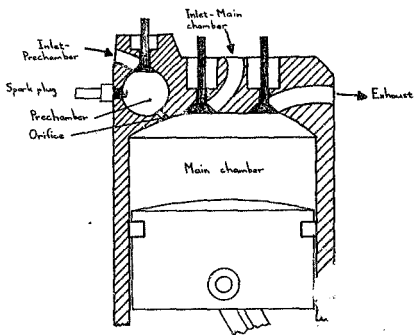


Figure 1 - Example of lean burn operation in engine with one prechamber

The above definitions cover many of the individual LB techniques or components being researched: pre-combustion chambers, flame torch ignition, high turbulence, swirl etc. Additional techniques that have been studied include high energy ignition systems, engine control by varying the overall AFR (rather than the flow rate of a mixture of constant AFR as in conventionally aspirated designs), pre-heating the incoming mixture (to improve mixture homogeneity), and direct fuel injection (to create an ignitable mixture around the spark plug). All present LB engine designs use a combination of some of the above techniques.

DESCRIPTION OF ENGINE

The research engine tested in this project is an extensively modified version of the Yamaha 55 BM, an outboard engine for marine applications. This is a two-cylinder, normally aspirated (two carburetors on the crankcase side) two-stroke engine having a rated maximum power of 40 kW and total swept volume of 750 cm^3 (bore x stroke = $82 \times 72 \text{ mm}$).

Lean burn operation was achieved by using one of the cylinders as a type of pre-combustion chamber. The crankshaft was modified so that both pistons move in unison, and the ignition system was altered such that both spark plugs fire together. A new single-piece aluminum cylinder head was manufactured, with disc type combustion chambers and centrally located spark plugs (Figure 2). The orifice allowing the flame torch from the pre-combustion chamber (called the mixture cylinder) to travel to the main chamber (called the air cylinder), is wide and shallow ($40 \times 2 \text{ mm}$), the cross-sectional area having been selected on the basis of the work of Hirako and Kataoka (2) by Neil and O'Brien (3). This orifice will henceforth be referred to as the inter-cylinder connecting (ICC) port. When assembled, the nominal and effective compression ratios of each cylinder were calculated to be 8:1 and 5.3:1 respectively. The carburetors were also modified to allow the AFR of each cylinder charge to be varied during operation by installing needles to throttle the main fuel jets.

Further modifications included the replacement of the standard magneto type ignition with a new system utilizing a standard breaker-point and cam system with no automatic advance. Thus, the ignition timing could be easily adjusted manually while the engine was running. The engine was mounted onto a test bed and aligned with a water brake dynamometer, power transmission being accomplished using a Fenner 130 HRC coupling. The engine thus lay on its side with the crankshaft in a horizontal position. Since the engine in the outboard motor form is mounted vertically, a redesigned carburettor inlet manifold was necessary for the present study.

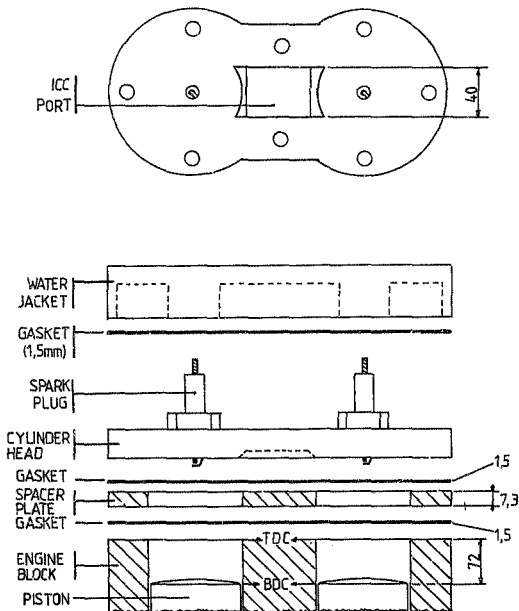


Figure 2 - Schematic of combustion chambers modified for lean burn operation (not to scale)

The gravity fuel feed system did not appear to be supplying fuel at a sufficiently high pressure. To solve this problem, and to allow fitting of a fuel filter into each line, two diaphragm electric fuel pumps were installed before each carburettor.

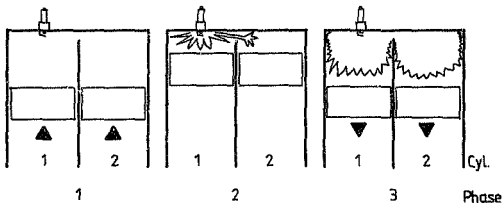


Figure 3 - Research engine: mode of operation

The anticipated mode of operation is shown in Figure 3. As both pistons travel towards top dead centre (TDC), each chamber has received its fresh charge pumped from the crankcase. During LB operation, cylinder 1 (the mixture cylinder) receives a close to stoichiometric mixture and cylinder 2 (the air cylinder) receives a very lean mixture (Figure 3, phase 1).

During phase 2, the contents of both cylinders are compressed to equal pressure and spark ignition occurs. However, the charge in the air cylinder is too weak to support combustion and only the mixture cylinder fires. The ICC port permits a torch of flame to propagate into the air cylinder thus igniting its charge.

Finally in phase 3, both cylinders travel towards bottom dead centre (BDC), expelling the burnt gases through the exhaust ports.

DESIGNS RELATED TO THE RESEARCH ENGINE

According to the engine classification method of Uyehara et al (4), the research engine is a reciprocating IC engine using the lean burn techniques with two homogeneous mixtures (one in each cylinder), direct spark ignition in the mixture cylinder, spark torch ignition in the air cylinder, and induction of the ignition mixture by a separate inlet manifold and valve (or transfer ports for a two-stroke) into the pre-chamber (the mixture cylinder).

This classification suggests that those designs most closely related to the research engine are the Honda CVCC and the Cranfield-Kushul engines.

The Honda CVCC

The Honda CVCC has now been in mass production for almost a decade. Each cylinder, in classic lean burn form, consists of a main and auxiliary combustion chamber with separate carburetors, intake passage and inlet valves (Figure 4). The auxiliary chamber contains the spark plug and is connected to the main chamber by an orifice (5).

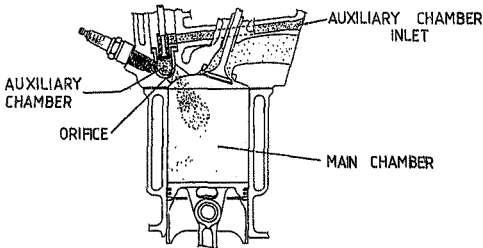


Figure 4 - Cross section of Honda CVCC engine (after Date et al)

The success of this engine is mainly dependent on the control of each mixture supplied to its respective combustion chamber. During suction, the relative control of each chamber's charge causes the transfer of some rich mixture to the main chamber, and during compression the transfer of some of the lean mixture from the main to the auxiliary chamber. Thus good combustion is achievable in the main combustion chamber by assuring stable ignition of the rich mixture in the auxiliary combustion chamber.

Measurements on this engine indicate a relatively high mean combustion temperature throughout the expansion stroke, which promotes the oxidation of CO and HC, and a relatively low peak combustion temperature in the main chamber, which minimizes NO formation.

The Cranfield-Kushul (C-K)

The C-K engine was originally invented by a Russian engineer V M Kushul in about 1965. Beale and Hodgetts (5,6) of the Cranfield Institute of

Technology presented two papers in the mid-1970's which reported tests on a Kushul-type engine based on a Rover four-stroke unit.

This engine, known as the Cranfield-Kushul, may be considered a complex version of our research engine. The major differences between the two are:

1. The C-K engine is a four-stroke engine.
2. The crankshaft of the C-K engine is offset by 20 to 30 degrees. This provides a two-stage transfer of charge across the ICC port.
3. Different volumetric CR's are used on each cylinder in the C-K engine.

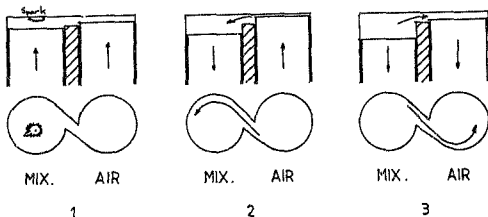


Figure 5 - Cranfield-Kushul engine: mode of operation (after Beale and Hodgetts)

Operation of the C-K engine involves three phases (Figure 5):

1. The mixture cylinder, leading the air cylinder, contains a combustible mixture that is ignited before the piston reaches TDC. At this position, the difference in compression ratios (9:1 in the mixture cylinder and 38:1 in the air cylinder) and the crankshaft phasing ensure that the gas pressure in each cylinder is independently equal.
2. The air cylinder now reaches TDC where its volume is a minimum. The pressure in the air cylinder is greater and its contents are transferred to the mixture cylinder via the inter-cylinder connecting (ICC) port, allowing a second stage of combustion.
3. The final stage of combustion occurs during the expansion phase of both cylinders. The burning gases now enter the air cylinder and combust in the remaining air.

The latest published information on this engine (7) dates from 1976. At that time, the leanest overall AFR that had been achieved was 50:1 at low loads. Most economical operation at low loads was found to occur at richer mixtures, namely at an AFR of 14:1. The engine could be operated at full air throttle on all loads, although it was found that slightly closing the mixture cylinder throttle created a stratification effect and delivered the best fuel economy. Emissions and specific fuel consumption of the C-K engine are highly competitive with those of the Honda CVCC, British Leyland BLML, Texaco and the Ford Proco designs.

Operation at an overall AFR as lean as 50:1 demands that high swirl be induced during the second phase of combustion. This was achieved by angling the ICC port (Figure 5). The effect of changing this port configuration was monitored by measuring the transient pressures in each cylinder and by noting the pressure differences and the onset of knock.

Both of the above engines differ from the research engine in some respects. The CVCC uses a fixed pre-combustion chamber of small volume as compared with the mixture cylinder of varying volume which also extracts work during operation. There is little difference in pressure before ignition occurs in the research engine, thus none of the advantages of lean and rich charge transfer across the ICC port, namely reduced emissions and improved combustion, are realised. The C-K, by using a deliberate phase difference between the cylinders and different volume compression ratios is characterised by a multi-stage charge transfer operation during which both a torch of flame and an unburnt lean mixture travel via the ICC port during one cycle.

Despite the less advanced design of the research engine, its performance should be compared with that of its closest relatives, namely the Honda CVCC and the Cranfield-Kushul designs.

INSTRUMENTATION OF THE RESEARCH ENGINE

Engine Input and Output

The fuel flow rate to each cylinder was determined using previously calibrated Pierburg (gear type) analogue fuel flow meters.

Total mass flow rate of air to the engine was obtained by measuring the pressure drop (by means of an electronic micromanometer) across an orifice plate fitted to an air surge reservoir, and by measurement of the inlet air temperature using a thermocouple.

The mechanical output of the engine was absorbed in a previously calibrated water brake dynamometer. Torque was read from a dial fitted to this instrument.

The engine speed was measured using a hand-held tachometer and mean exhaust pressure was read from a water manometer.

Transient parameters

The most important of these was combustion chamber pressures. Both cylinder heads were fitted with Kistler 6121A1 piezo-electric pressure transducers enclosed in water cooling jackets. The output signals of the transducers were converted into voltages using charge amplifiers, and fed to a six channel Datalab transient recorder. Pressure versus time traces for either single or multiple engine cycles could be obtained by varying the recorder's sample rate. The traces were displayed on an oscilloscope and fed to an HP9816 computer for data storage and processing.

The transient recorder was triggered with the pistons at TDC, the triggering signal being obtained from an optical emitter-sensor unit bracketed to the engine. A voltage comparator circuit supplied a 5 V triggering step to the recorder whenever the normally interrupted light path of the optical sensor was rendered continuous. This was achieved via a slit cut into a disc fitted to the crankshaft. Adjustment of the optical sensor bracket to ensure triggering at TDC was achieved by motor-

ing the engine at constant speed and ensuring that the TDC marker coincided with the peak pressure of both combustion chambers.

The above pressure records and the TDC signal were used to monitor the combustion process and the onset of knock.

In order to balance the inlet quantities of fresh charge into each cylinder, a Kistler piezo-electric differential pressure transducer was installed across one transfer port for each cylinder. This was necessary since only one air reservoir was available and this supplied air to both cylinders. Hence, flow rates to each cylinder were measurable only when they were equal. Brass taps were installed between the transfer ports and the transducer, which were closed after balancing for fear of endangering the transducer in case of engine backfire. The output from this transducer was also fed to the transient recorder via a charge amplifier.

The above three pressure records and the TDC signal occupied four channels of the recorder. The fifth channel was used to record the instant of spark discharge through the leads. The spark plug leads were passed through a current transformer, the output from which was stepped down before feeding to the recorder input.

Output Plots

The plots available from the menu driven computer program were:

1. Pressure-time trace in the mixture cylinder
2. Pressure-time trace in the air cylinder
3. Superimposed traces of 1 and 2
4. Differential pressure - time trace (mixture cylinder less air cylinder)
5. Inlet differential pressure across transfer ports
6. Ignition timing

RESULTS AND DISCUSSION

The engine ran for approximately five hours in total. However, the lack of primary reciprocating balance of the pistons and connecting rods caused heavy vibration. Even with the engine, coupling and dynamometer accurately aligned under static conditions, the vibration led to instantaneous misalignment beyond the coupling's specified limit. This in turn caused overheating of the coupling which severely hampered testing. Also, a more extensive testing period would almost certainly have resulted in the destruction of some component of the engine or test rig.

The lowest achievable speed of the engine at minimal load (approximately 5 Nm due to friction within the dynamometer) was 800 rpm. The occurrence of only one combustion period per engine cycle, owing to the in-phase, rather than 180° out of phase operation, probably accounts for this slightly high idling speed.

Only one common air inlet measurement system was fitted to the engine. Thus quantitative information on AFR's was obtainable only with equal air flow rate to each cylinder. The air flows could be balanced by adjusting the throttles for zero (or minimal) pressure difference between the inlet transfer ports of the two cylinders.

With equal air and fuel flow to each cylinder, the maximum speed at minimum load was 2000 rpm. On applying load (still with balanced air and fuel flows) the maximum achievable power was 2.9 kW (23 Nm at 1200 rpm). The corresponding brake thermal efficiency was 4.3%. In either of the above cases, further opening of the throttles caused misfiring. This could not be corrected by adjusting the ignition timing.

The engine ran on extremely rich mixtures only, with AFR's of 6:1 or less for both cylinders. Since such values are normally beyond the rich limit of running, the exhausting of unburnt fuel was indicated. This was confirmed by the presence of excessive quantities of two-stroke lubricant in the exhaust.

Such overall incomplete combustion can be caused either by intermittent firing cycle-to-cycle, or by consistent firing, but with incomplete combustion in each cycle or by a combination of these. Figure 6 showing typical consecutive combustion chamber pressure traces, provides clear evidence of intermittent combustion. The lower pressure peaks occur at 8 bar (gauge), the value corresponding to the previously determined 'motoring' (compression without ignition) pressure peaks.

It is strongly suspected, however, that even on firing, combustion was incomplete. The reason for this overall incomplete combustion may be examined in terms of mixture inhomogeneity. Ultimately, homogeneity is required within the combustion chamber. It can be brought about both during the carburation and inlet processes, and by events occurring within the combustion chamber itself.

Since the carburetors and inlet system did not differ radically from those of the engine in original form (which clearly ran satisfactorily), the reasons for mixture inhomogeneity must be associated with the nature of the (modified) combustion chamber. The design of a combustion chamber, greatly affects the level of turbulence generated during compression. Two-stroke engine designs always use squish bands to generate turbulence towards TDC. The research engine's combustion chambers are of the disc type with centrally located spark plugs and convex crowned pistons, which, featuring neither squish bands nor a turbulence inducing cavity, are clearly not conducive to turbulence generation.

Further, the combination of the flat cylinder heads and the crowned (convex upwards) pistons, constitutes a weak squish region with flow away from the spark plug. Thus, the major portion of the mixture, together with whatever weak turbulence is generated, resides at the most unfavourable position, namely at the quench-prone circumference of the cylinder head.

Clearly the combustion chamber design is totally unsatisfactory. Some improvement in combustion might however be possible by increasing the

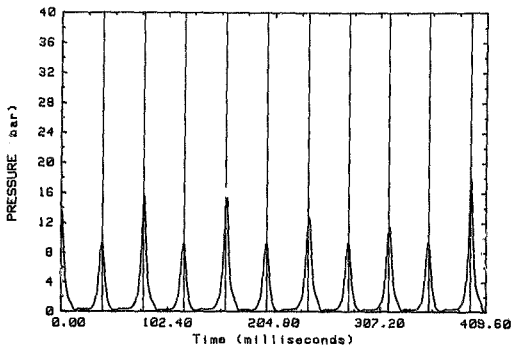


Figure 6 - Pressure versus time trace: mixture cylinder

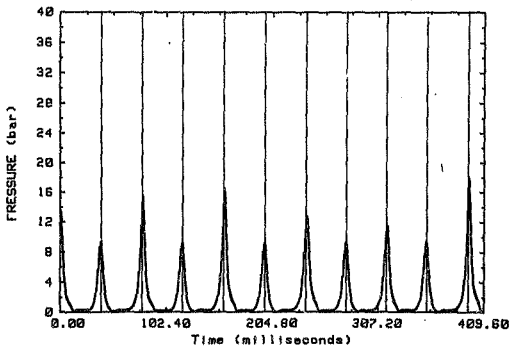


Figure 7 - Pressure versus time trace: mixture and air cylinders

mixture homogeneity externally, for example by means of heating the inlet manifold. While this process lowers volumetric efficiency, this is outweighed by the resulting improved combustion (8).

It is conceivable that the expulsion of unburnt mixture was in part associated with the physical orientation of the engine: that is, with the cylinder axes lying horizontally and the exhaust ports facing downwards. Gravity, and the flow patterns created by the pistons rising from BDC, might thus assist in accelerating the densest portions of the mixture towards the exhaust port.

No evidence of knock was detected, even with the ignition timing advanced to 50° BTDC. This constitutes further evidence of inefficient combustion.

Figure 7 shows superimposed multiple pressure traces for both cylinders. It should be observed that while sharp cycle-to-cycle pressure differences (misfiring and firing) occurred, these took place simultaneously and with virtually identical magnitude in both cylinders. It would thus appear that the two combustion chambers were not behaving independently. This was confirmed by attempts to lean out the air cylinder, which still resulted in identical pressure traces in both cylinders. In effect, the two cylinders were behaving as one. This would imply that the ICC port had too large a cross-sectional area. In addition, the flat shape of the port exposed a large and potentially quenching surface area to the flame torch, if the engine were to run as originally intended.

CONCLUSIONS AND RECOMMENDATIONS

The main conclusions of this study are:

1. The test engine vibrates badly owing to lack of primary reciprocating balance.

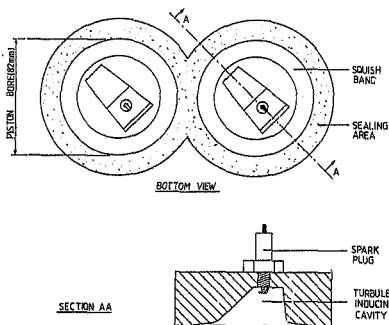


Figure 8 - Schematic of original Yamaha 55BM cylinder head

2. The presence of a single air flow measuring system limits testing to cases of equal air flow into each cylinder.
3. Combustion was inefficient and intermittent, owing to the inhomogeneity of the incoming mixture, poor combustion chamber design, and possibly the physical orientation of the engine cylinders.
4. The design of the ICC port is unsatisfactory.

In view of these findings the following recommendations are offered:

1. If the present engine is to remain in use at all, that the test bed be rebuilt, fitting both dynamometer and engine to a common rigid base and replacing the coupling with one tolerating greater misalignment.
2. That the engine (if retained) be repositioned such that the exhaust ports lie along the upper area of each cylinder.
3. That an alternative engine be considered which may be modified to have two adjacent cylinders interconnected and in phase while retaining primary reciprocating balance. In the case of an in-line four-cylinder

engine, for example, the central two cylinders would become the mixture and air cylinders and the outer two, moving in phase with each other, but 180° out of phase with the former, would be non-combusting balancers. The crankshaft of such engines would not require modification. In the case of two-stroke engines, the outer cylinders would require special lubrication.

4. That separate air flow measuring systems be installed for each combustion cylinder.
5. That the combustion chambers be designed to incorporate squish bands and cavities to induce turbulence, the latter being situated in close vicinity to the spark plugs. A design similar to that of the Yamaha 55 BM in original form is suggested (Figure 8).
6. That consideration be given to homogenizing the incoming mixture by heating the inlet manifold.
7. That both the cross-sectional and the surface areas of the ICC port be reduced. Provision for varying the size of port during testing would be highly desirable.

ACKNOWLEDGMENTS

The author offers his thanks to the following:

- * Mr R M Amm for making available an early version of the lean burn engine which was the subject of this study
- * The Anglo American Corporation of South Africa for financial contribution to this project
- * The Council for Scientific and Industrial Research for providing a bursary for postgraduate study
- * Professor C J Rallis, Dr H H Jawurek and Mr N W Lane for guidance and enthusiastic participation throughout this project.

REFERENCES

1. Germano G J, Wood C G and Hess C C (1983) Lean combustion in spark-ignition internal combustion engines - a review SAE Paper 831694 presented at the Fuels and Lubricants Meeting, San Francisco, California October 31 - November 3, 1983, 20pp
2. Kataoka K and Hirako Y (1982) Combustion process in a divided chamber spark ignition engine Bulletin of the JSME Paper 210-13, Vol 25, December 1982, 8pp
3. Nel G W and O'Brien T M (1984) Commissioning of a two-stroke two-cylinder lean burn engine Final year research project, Mechanical Engineering, University of the Witwatersrand
4. Uyehara D A, Myers P S, Marsh E E and Cheklich G E (1974) A classification of reciprocating engine combustion systems SAE Paper 741156 presented at the International Stratified Charge Engine Conference, Troy, Michigan October 30 - November 1, 1974, 8pp
5. Date T, Yagi S, Ishizuya A and Fujii I (1974) Why the Honda CVCC Engine meets 1975 emission standards Automotive Engineering Vol 82, No 9, pp 50-55 (Based on SAE paper 740605 Research and development of the Honda CVCC engine)
6. Beale M R and Hodgetts D (1976) Further progress in the development of the Cranfield-Kushul engine SAE Paper 765024 6pp
7. Beale M R and Hodgetts D (1975) The Cranfield-Kushul engine Paper C90/75 accepted for publication by the Institution of Mechanical Engineers on 18th March 1975, London pp87-95
8. Harrow G A and Clarke P H (1979) Mixture strength control of engine powers: Fuel economy and specific emissions from gasoline engines running on fully vaporized fuel/air mixtures Paper C90/79 in IMechE conference

publications 1979-9 Fuel economy and emissions of lean burn engines,
pp 39-50 Mechanical Engineering Publications Limited, London

APPENDICES

For the purpose of all appendices, the following abbreviations are used:

AFR	Air-fuel ratio
BDC	Bottom dead centre
CI	Compression ignition
CO	Carbon monoxide
CR	Compression ratio
HC	Hydrocarbons
IC	Internal combustion
LB	Lean burn
MBT	Maximum best torque
NO _x	Oxides of nitrogen
SC	Stratified charge
SI	Spark ignition
TDC	Top dead centre

APPENDIX A

LEAN BURN ENGINES: A GENERAL INTRODUCTION

The purpose of this Appendix is to provide a background to the field of lean burn/stratified charge engines in general and to the transfer-port type of engine being tested in this project in particular.

A.1 Definition of Lean Burn Engines

Lean burn reciprocating internal combustion engines operate with an overall air-fuel ratio considerably weaker than conventional engines. Numerous methods are used to allow operation beyond the lean misfire limit of conventional engines.

A.2 The Need for Lean Burn Engines

The two major reasons for finding a replacement for conventional spark ignition engines are emission control and fuel consumption - the need to reduce both the quantity of fossil fuel being consumed worldwide, as well as the quantity of noxious by-products of the energy conversion process.

It is common knowledge that the automobile is a major contributor to the high hydrocarbon (HC), oxides of nitrogen (NO_x) and carbon monoxide (CO) levels in urban areas. Both Stirling and lean burn/stratified charge engines have come into consideration as suitable replacements (1)

Production or near production examples of lean burn engines already exist; examples include the Honda CVCC, Ford Proco, Jaguar XJS (May Fireball) and the Porsche SKS and SC.

The process of formation of emission pollutants within the engine are described in the next section. However it should be noted that consider-

able hydrocarbon vapour emissions occur in other areas, such as the fuel tank, carburettor and crankcase vents (2), where fuel and lubricant are able to evaporate.

Apart from the reduced emission of pollutants, lean burn/stratified charge techniques hold additional advantages. These include:

1. Improved thermal efficiency resulting from increasingly lean mixtures. The improvement is related to three effects which result from the lower combustion temperatures with lean mixtures, namely the increased specific heat ratio, the reduced dissociation losses and the reduced heat transfer to the combustion chamber walls.

Lean burn techniques also allow engine operation at higher compression ratios, due to extending of the lean misfire limit. This also results in improved thermal efficiency, since for the air standard Otto cycle:

$$\eta_t = 1 - (1/r)^{\gamma-1} \quad \text{where } r = \text{compression ratio}$$

$\gamma = \text{ratio of the principal heat capacities } c_p \text{ and } c_v$

2. Elimination of expensive catalytic converters in the exhaust system, which have become necessary in conventionally powered automobiles to meet the strict emission control measures - particularly in the United States.

3. Reviving interest in the 2-stroke cycle engine. Various researchers, especially Onishi and Fujii of the Nippon Clean Engine Research Company have discovered that 2-stroke engines have greater potential for emission reduction with lean burn operation.

The factors which in the past often discouraged production plans for lean burn engines were the unstable operation due to erratic combustion and misfire, and the previously cheap and plentiful supply of crude oil.

A3 The Formation of Pollutants

Figure A1 shows the three processes of pollutant formation within a conventional 4-stroke spark ignition engine.

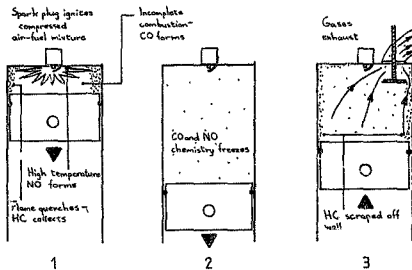


Figure A1 - Pollutant formation within an engine

During the first stage, the ignition of a compressed air-fuel mixture creates high temperatures and a propagating flame front. As the flame approaches the cylinder walls, quenching occurs due to the lower wall temperature, and a thin layer of unburnt mixture and hence hydrocarbons adhere thereto. In addition, unburnt mixture accumulates above the piston ring between the piston and wall. Nitric oxide and carbon monoxide also form during the first stage as a result of the high combustion temperatures and incomplete combustion.

During the second stage, the falling bulk-gas temperature created by gas expansion prevents the completion of oxidation reactions from occurring.

The final stage exhausts the nitric oxide, carbon monoxide, and the hydrocarbons (which are scraped off the cylinder walls as the piston travels upwards to top dead centre).

This basic description, coupled with the knowledge that lean mixtures attain lower maximum combustion temperatures suggest the potential of lean burn/stratified charge engines in reducing NO and CO emissions.

In addition, suitable design of the engine itself can lead to reduced mixture quenching on the cylinder walls and reduced HC emissions. Examples of such designs would incorporate use of pre-combustion chambers or swirl techniques.

A.4 Techniques of Achieving Lean Burn/Stratified Charge Operation

In the foregoing, the terms 'lean burn' and 'stratified charge' have been used. Both techniques have the same objective (that is, low emissions resulting from lean overall mixtures), but the methods to achieve this do differ somewhat. Certain engine designs utilize both 'lean burn' and 'stratified charge' techniques, so the border is not clearly defined.

Lean burn engines generally utilize a finite number of homogeneous mixtures of different air-fuel ratios (AFR's). That number may range from one to three. In a typical lean burn engine, a rich mixture is ignited in a pre-combustion chamber and the flame front subsequently propagates into the main chamber (via an orifice) which contains a weaker mixture (Figure A2). Other examples use one weak mixture only with no prechamber, but generate very high turbulence to guarantee reliable ignition. To supplement this, direct fuel injection towards the spark plug region has also been used.

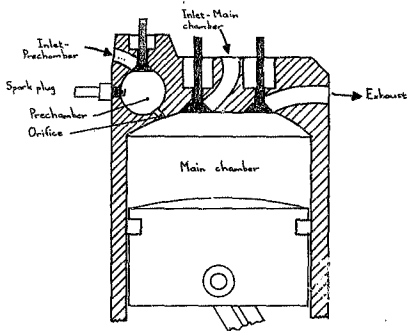


Figure A2 - Example of lean burn operation in engine with one prechamber

The stratified charge engine creates a continuous gradient of varying air-fuel mixtures in all three dimensions based on density differences. No physical boundary exists between these layers, and the process is often improved by careful design to achieve swirl of the incoming mixture.

Uyehara et al (3) derived a classification system for reciprocating internal combustion engines, and placed each lean burn engine existing at that time (1974) into distinct groups (Figure A3)

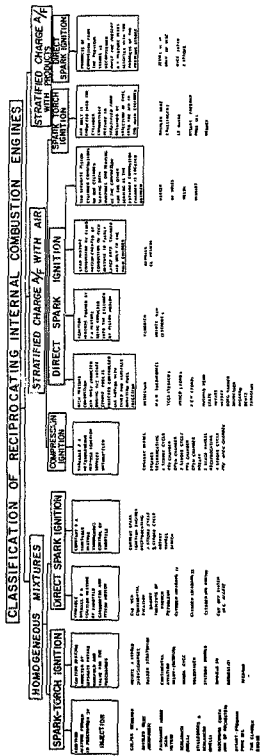


Figure A3 - Classification of reciprocating IC engines

This large field was first divided into lean burn (that is, distinct homogeneous mixtures) and the stratified charge fields. The following subdivisions considered the mode of mixture ignition—either direct spark or torch ignition (using a pre-combustion chamber). Finally, most subsystems separate the induction of the richer mixture into the engine—either by additional fuel injection into the first region to ignite, or by separate introduction through a second inlet system.

Further explanations of the physical appearance and operation of some of the engines bearing the closer similarity to the research engine tested are discussed in Appendix B.

A.5 Introduction of the Research Engine of this Study

The research engine tested in the University of the Witwatersrand Mechanical Engineering Laboratory was kindly supplied by Mr R M Amm of Durban. Originally, the engine was a 40 kW (approximately 750 cc) Yamaha outboard engine of parallel 2-cylinder, 2-stroke configuration with a 180° offset crankshaft.

The engine has been modified for lean burn operation as follows:

1. The crankshaft has been rebuilt such that both pistons move in phase.
2. A new cylinder head with an inter-cylinder connecting port has been fitted.
3. The carburettor systems have been modified to allow the air-fuel ratio in each cylinder to be varied separately during operation.
4. The ignition system has been modified to allow simultaneous firing of both cylinders.

A fuller description of all modifications and instrumentation is provided in Appendix C and D.

The anticipated mode of operation is shown in Figure A4.

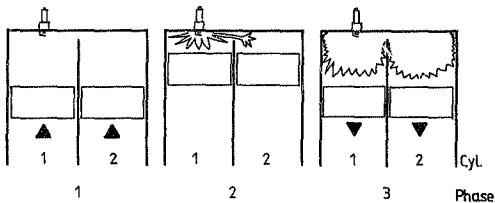


Figure A4 - Mode of operation of the research engine

As both pistons travel towards top-dead centre (TDC), each chamber has received its fresh charge pumped from the crankcase. During lean burn operation, cylinder 1 receives a close to stoichiometric mixture, and cylinder 2 a very weak mixture (Phase 1). For brevity, cylinder 1 is referred to as the 'mixture' cylinder and cylinder 2 as the 'air' cylinder throughout.

During phase 2, the contents of both cylinders are compressed to equal pressure and spark ignition occurs. However, the charge in the air cylinder is too weak to support combustion, and only the mixture cylinder fires. The inter-cylinder port permits a torch of flame to propagate into the air cylinder thus igniting its charge.

Finally in phase 3, both cylinders travel towards bottom dead centre (BDC), expelling the burnt gases through the exhaust ports.

The spark plug in the air cylinder was retained in order to assist in starting the engine with equally rich air-fuel ratios in each cylinder.

A.6 Classifying the Research Engine

The general classification of the research engine was carried out, using the system of Ueyehara et al (3), in order to discuss the more closely related engine designs already produced in the literature survey. Even so, each specific engine exhibits its own unique properties and performance, and it is thus difficult to make any predictions with regard to the research engine from the work of others.

The stages in classifying our engine according to the nomenclature of Figure A3 are as follows:

1. Reciprocating internal combustion engine.
2. Homogeneous mixtures (Two, one in each cylinder)
3. Direct spark ignition (in mixture cylinder).
4. Spark torch ignition (in air cylinder)
5. Ignition mixture inducted by separate intake manifold and valve (or transfer port for 2-stroke cycle engines) from the prechamber (the mixture cylinder).

According to his analysis, our research engine falls into the same category as the Honda CVCC and the Volkswagen lean burn engines, although the prechamber is a cylinder of varying volume. Another related concept is the Cranfield-Kushul engine. Its configuration is very similar to the research engine, except that the mixture cylinder leads the air cylinder by twenty to thirty degrees crankangle. This, and the different volumetric compression ratios of each cylinder, facilitate a multi-stage charge transfer mechanism, where either a torch of flame or an unburnt air-fuel mixture travels via the inter-cylinder connecting port during an engine cycle.

A10

It is these types of engine which are discussed in further detail in Appendix B.

APPENDIX B

SURVEY OF LITERATURE

The literature survey presented below deals with petrol-fuelled, reciprocating LB SI engines, and, in view of our test engine, emphasis is placed on normally aspirated rather than direct fuel injected machines.

The classification technique of Uyehara et al (3) was applied in Appendix A (p A9), and on this basis, engines and aspects of design which are related to the research engine are summarized in Figure B1.

The major source of information in this survey was the Society of Automotive Engineers (SAE), using the SAE database of the ORBIT system sold by SDC in Santa Monica, California, USA. It was accessed telephonically via the on-line facility at the Wartenweiler Library, University of the Witwatersrand, using the key-words 'lean burn', 'stratified charge' and 'Cranfield-Kushul'. Copies of the abstracts thus obtained supplement one copy of this report, and are on file in the School of Mechanical Engineering. From this broad spectrum of papers, those more relevant to our test engine (and emphasising performance rather than emission characteristics) were ordered, and are also on file in the School.

Other sources of information included the General database of the Dialog database sold by Lockheed Aircraft, Palo Alto, California, USA. This database supplied references to publications such as 'Automotive Engineering' (USA), 'Automotive Engineer' (UK), the 'Bulletin of the Japanese Society of Mechanical Engineers', and Conference Proceedings of the Automobile Division of the Institution of Mechanical Engineers (London).

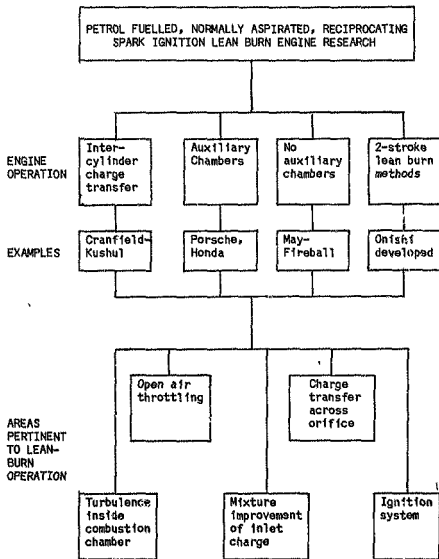


Figure B1 - Classification of research engine and related designs

This survey is presented under the following headings:

- B.1 Introduction to lean burn engines
- B.2 Engine designs related to the research engine
- B.3 Specific areas of study
- B.4 Miscellaneous

B.1 Introduction to Lean Burn Engines

A number of SAE papers can be recommended as suitable introductions of the lean burn/stratified engine field.

The approach towards reciprocating engine classification used by Uyehara et al (3) covers all aspects of LB operation. The classification (Appendix A, p A6), however, does not include the later designs by May (Fireball head), Porsche (SC) or Kuschl (Cranfield-Kuschl). The research engine, as classified in Appendix A, falls into the categories of 'homogeneous mixture', 'normally aspirated', 'LB reciprocating IC engine', and utilizes both direct spark and spark-torch ignition. Designs by Honda (CYCC), Nilov and Volkswagen would also appear to be related to the research engine. The main characteristics in this category are low NO and CO emissions, higher than normal HC emissions, and the difficulty of maintaining reasonably short combustion times for mixtures of AFR beyond 25:1.

Dartnell (4) studied the inevitable trade-off between fuel consumption and emissions in terms of engine compression ratios. The trends in compression ratios in US cars was a decrease from an average of 9.4:1 in 1970 to 8.25:1 in 1975 (Figure B2) to permit operation with an unleaded fuel of lower octane number. The resultant increase in fuel consumption represented 3.5% of the total US oil requirements in 1978. He views the May Fireball as a solution to the trade-off - a high compression ratio design (typically 14:1) operating with normal premium fuel and very high turbulence levels to permit rapid burning of lean mixtures.

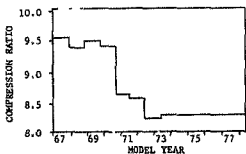


Figure B2 - Trend in compression ratios of US cars

Germane et al (5) provide, from a most comprehensive reference source, a review of the fundamentals of lean combustion and of the effect of lean mixtures on engine efficiency, performance and exhaust emissions. The techniques for lean burn engine control are also discussed. This, coupled with a thorough treatment of the theory of all aspects of lean burn operation provides a highly recommended introductory paper.

Hartley (6) reviews methods of achieving consistent combustion of lean mixtures. The design of modified induction manifolds (Figure B3), dual ignition systems and high compression combustion chambers (as in the May Fireball and the Porsche SC engines) are discussed.

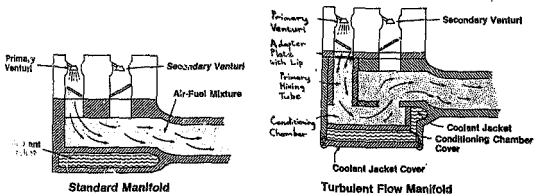


Figure B5 - Comparison of turbulent flow manifold with standard intake manifold

B.2 Engine Designs Related to the Research Engine

These will be discussed under the following headings:

- B.2.1 Honda CVCC
- B.2.2 Porsche SC
- B.2.3 Staged Combustion Compound Engine (SCCE)
- B.2.4 Two-stroke LP designs
- B.2.5 May Fireball
- B.2.6 Cranfield-Kushul

B.2.1 The Honda Compound Vortex Controlled Combustion (CVCC) engine

Date et al (7) of Honda Research, provide a comprehensive explanation of the CVCC's operation, which has now been mass produced for a number of years.

Each cylinder consists of a main and an auxiliary combustion chamber with separate carburetors, intake passages and inlet valves. The auxiliary chamber contains the spark plug and is connected to the main chamber by an orifice (Figure B4).

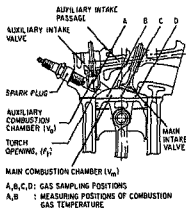


Figure B4 - Sectional view of Honda CVCC cylinder

The success of this engine depends mainly on the control of each mixture supplied to its respective combustion chambers. During suction, the relative control of each chamber's charge causes the transfer of some rich mixture to the main chamber, and during compression the transfer of some of the lean mixture from the main to the auxiliary chamber.

Measurements on this engine indicate a relatively high mean combustion temperature throughout the expansion stroke, which promotes the oxidation of CO and HC, and a relatively low peak combustion temperature in the main chamber, which minimizes NO formation (Figure B5). Partial inter-cylinder charge transfer prior to ignition may occur in our research engine as well; thus a comparison of combustion chamber pressure diagrams for the two engines (under similar operating conditions) would be of interest.

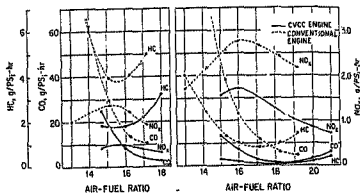


Figure B5 - Exhaust gas emissions of CVCC engine and a conventional engine at idling (isfc = 410 g/PS-hr)

B.2.2 The Porsche stratified charge (SC) engine

The Porsche SC engine (8) utilizes two auxiliary chambers per cylinder, each fitted with a fuel injector (Figure B6). Initial ignition occurs in the first auxiliary chamber furthest from the main chamber, which is relatively turbulence free.

The advantage of this design lies in the fact that the combustion process can be controlled to release 85% of its energy near TDC.

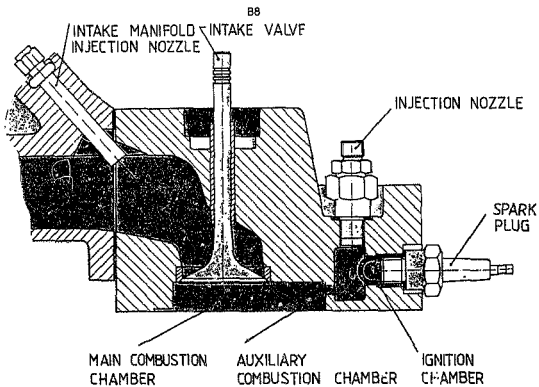


Figure B6 - Cross-section of Porsche SC cylinder.

This improvement in the combustion process has been found to lead to reduced sensitivity to changes in CR, fuel characteristics, AFR and ignition timing. In addition, the engine operates with a high degree of stability across a wide speed and load range, and the emission characteristics are considerably improved in comparison with a conventional Otto cycle engine (Figure B7).

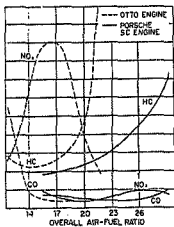


Figure B7 - Exhaust emissions of Porsche SC engine compared with conventional engine

Various types of Porsche LB engines exist, some using direct fuel injection, while others use a separate intake to the auxiliary chambers. In addition, other designs such as a high CR LB engine have also been developed (9).

B.2.3 The staged combustion compound engine (SCCE)

Stewart and Turns (10) present the SCCE engine which employs pairs of cylinders (as in our research engine), but these are offset by 180° of crank angle (Figure B8).

B10

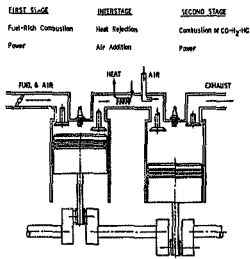


Figure B8 - One staged combustion compound engine

The first cylinder of each pair aspirates and burns a homogeneous fuel-rich mixture. The exhaust gases, containing quantities of combustible products (CO, HC and H₂) and a small quantity of NO_x are cooled (to suppress knock), mixed with additional air and combusted in the second cylinder. Additional work is extracted during this second phase and the combustion products are reduced further while maintaining low NO_x concentrations. The division of fuel energy between the two phases is considered to be fundamental to the process.

No further information regarding the SCCE is available. Test results of a V-8 prototype indicated that it was not possible to meet US emission control specifications without a catalytic converter. This, coupled with the need to increase the engine displacement by 40% in order for its power output to equal that of conventional engines, probably removes it from serious consideration. Nevertheless, the use of coupled cylinders, as with our research engine, prompts the idea of using multiple pairs of cylinders, such as a flat four engine in future projects.

B.2.4 Two-stroke cycle lean burn designs

Since our research engine is of the two-stroke type, all available literature relating to such lean burn operations was acquired. If the traditional disadvantages of a two-stroke engine (high emissions at part load, high fuel consumption and erratic operation at low load) can be overcome, the advantage of simple construction and high performance per unit volume could still be retained.

Until recently, the attention devoted to measuring power output and the subsequent use of cylinder port areas has caused the above disadvantages. This is due to increased blow-by into the exhaust passages at high engine speeds.

A further number of differences between conventional two and four-stroke engines exist (11):

Trapping efficiency

Figure B9 relates the effects of equivalence ratio on the thermal efficiency of a fuel-air cycle as a function of trapping efficiency. With conventional two-stroke cycle engines the trapping efficiency lies between 0,6 and 0,7, while with four-stroke engines the thermal efficiency is almost equal to a trapping efficiency of unity. Thus the thermal efficiency of conventional two-stroke cycle engines is lowered by its low trapping efficiency.

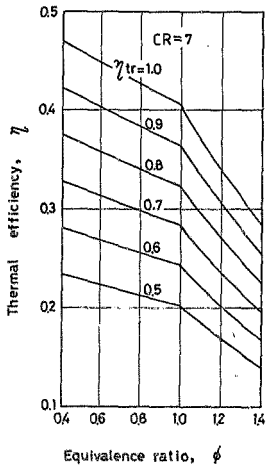


Figure B9 - The effect of trapping efficiency on fuel-air cycle thermal efficiency

Lean combustion

Figure B9 also indicates the improvement in thermal efficiency that is obtainable by using lean mixtures.

A two-stroke engine has advantages for operation close to the lean limit, namely the existence of high temperature residual gases, turbulent flow caused by scavenging flows, and a wide freedom in deciding on the shape of the combustion chamber.

Losses

Important noticeable characteristics of two-stroke engines are the reductions in mechanical, heat and pumping losses. These result from the mechanical simplicity and absence of valve driving mechanisms, and from the compactness of the combustion chambers. Two-stroke engines have low pumping losses at part-throttle loads (contrary to four-stroke engines) and this characteristic partially accounts for their unstable combustion at part load.

Yui and Onishi (12) developed their combustion process for a fuel injected two-stroke engine. All three toxic pollutants are controlled and performance is improved by deliberately retaining a proportion of the exhaust gases in the engine using controlled swirl (Figure B10).

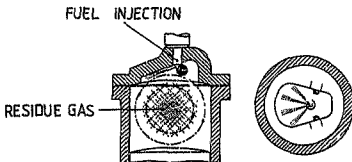


Figure B10 - YOCP process. Cylinder head showing residue gas

They suggest that by such means the traditional disadvantages of two-stroke engines are removed, and that fuel consumption, specific power output and engine response are superior to those of a four-stroke engine.

Yui and Onishi's paper was presented in 1969 and no further work of the YOCP process appears to have been published. In 1984 however, Onishi et al (11) presented a study on the Multi Layer Stratified Scavenging (MULS) process. Two methods of stratifying two-stroke engine charges may be employed:

1. Combusted gas exists before a fresh charge is introduced (eg unflow scavenging).
2. Prevention of the rich mixture from escaping by stratification of it with air or a lean mixture (eg engines with double air inlets and transfer ports).

The MULS process follows method 2, but uses a single air inlet (Figure B11). It was found that the incoming mixture was always heterogeneous. Thus, if the mixture was introduced towards the wall opposite the exhaust port, the density and phase differences between the unmixed fuel and air resulted in stratification occurring.

The above techniques suggested that it is possible to introduce a number of air-fuel mixtures of varying concentrations through separate scavenging ports and allow more precise control of the combustion process (Figure B11).

815

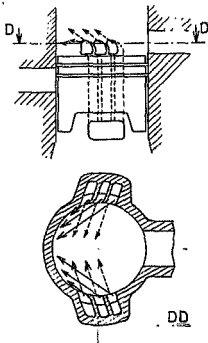


Figure B11 - MULS engine scavenging

The results of this study indicates that the MULS engine approach displays the following desirable characteristics:

1. Improved thermal efficiency and brake specific power output.
2. Reduced HC and NO_x emissions.
3. Applicability to any two-stroke engine irrespective of size, load conditions or purpose.
4. Mechanical simplicity.

Additional information on this system would be desirable. The heterogeneity of the inlet mixture using a normal carburettor is of some concern in the research engine as well, since, in its present location, the exhaust ports lie at the base of the sleeves (Appendix C). A proportion of the heavy, fresh rich mixture region could be pumped through directly into the exhaust.

B.2.5 The May Fireball head

The design of May (13) is not directly related to the research engine, but serves as a fine example of high compression L₁₃ operation using deliberately high induced turbulence within the engine. Such a technique could also be of use in future development of the research engine.

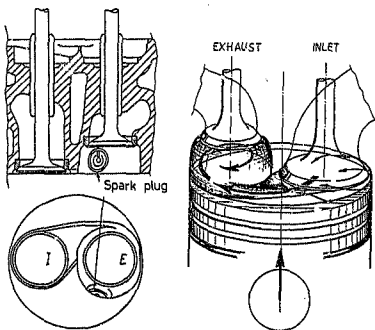


Figure B12 - The May Fireball combustion chamber

May followed a process of elimination in his search for a combustion chamber permitting high compression ratios. He considered the use of the bowl-in-piston design and the advantages of constraining combustion to occur beneath the hot exhaust valve only before finally recommending the Fireball chamber (Figure B12).

The spark plug is located on the side of the actual combustion chamber, and ignites the highly turbulent inlet mixture. Turbulence is squish induced using an eccentric connecting channel.

Results using CR's as high as 14.6:1 indicate most efficient operation at AFR's or 18 to 20:1. All three pollutants are reduced to the same extent as in the Honda CVCC, but the fuel consumption is significantly better (Table B1) than either the Honda or a conventional engine prior to the Fireball conversion.

Table B1 - Car data: May Fireball vs standard engine and Honda CVCC

General data			
Car type	VW Passat Variant Standard	VW Passat Variant May Fireball	Honda CVCC Standard
Model year	1974	1974	
car weight (kg)	910	910	730
engine capacity (cm ³)	1470	1470	1488
compression ratio	9,7 : 1	14,8 : 1	7,7 : 1
output PS DIN	65	90	63
cylinders	4	4	4
fuel required ROZ	97	97	91
ECE Test			
emissions HC gr/test	3,11	2,58	1,4
CO	80,4	20,0	17,8
NOx	6,14	2,0	2,6
ECE Test			
consumptions MPG	19,67	29,0	19,0
1/100 km	11,97	8,1	12,58
% reduction	100 %	-32 % -35 %	100 %

B.2.6 The Cranfield-Kushul (C-K) engine

The earliest publication relating to this engine was in a Russian textbook published in Leningrad in 1965 by V M Kushul. Beale and Hodgetts (14,15) presented two papers in the mid-1970's after conducting tests with a suitably modified Rover engine at the Cranfield Institute of Technology.

The C-K engine may be considered as a complex version of the research engine. The major differences between the two are:

1. The C-K engine is a four-stroke engine.
2. The C-K's crankshaft is offset by 20 to 30 degrees. This provides a two-stage transfer of charge.
3. Different volumetric CR's are used on each cylinder in the C-K engine.

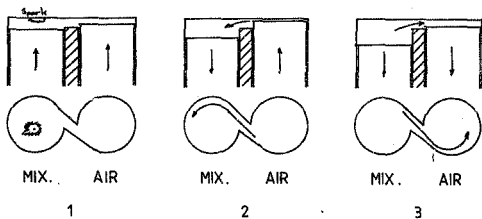


Figure B13 - Cranfield-Kushul engine operating phases

Operation of the C-K engine involves three phases (Figure B13).

1. The mixture cylinder, leading the air cylinder, contains a combustible mixture that is ignited before the piston reaches TDC. At this position, the difference in compression ratios (9:1 in the mixture cylinder and 38:1 in air cylinder) and crankshaft phasing ensure that the gas pressure in each cylinder is independently equal.
2. The air cylinder now reaches TDC where its volume is a minimum. The pressure in the air cylinder is greater and its contents are transferred to the mixture cylinder via an inter-cylinder connecting (ICC) port, allowing a second stage of combustion.
3. The final stage of combustion occurs during the expansion phase of both cylinders. The burning gases now enter the air cylinder via the ICC port and combust in the remaining air.

The latest published information on this engine (15) dates from 1976. At that time, the leanest overall AFR that had been achieved was 50:1 (by mass) at low loads. Most economical operation at low loads was found to occur at richer mixtures, namely at an AFR of 26:1. The engine could be operated at full air throttle on all loads, although it was found that slightly closing the mixture cylinder throttle created a stratification effect and delivered the best fuel consumption. Emissions and specific fuel consumption of the C-K engine are compared in Figures 14-17 with those of the Honda CVCC, the British Leyland BLML, the Texaco and the Ford Proco designs. All engines were adjusted for minimum emissions, while the C-K was also adjusted for minimum fuel consumption.

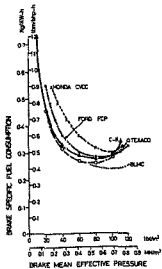


Figure B14 - Variation of the brake specific fuel consumption with brake load

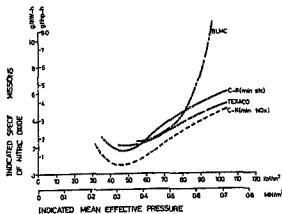


Figure B15 - Variation of NO emissions with indicated load

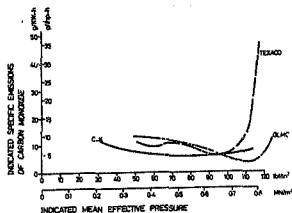


Figure B16 - Variation of CO emissions with indicated load

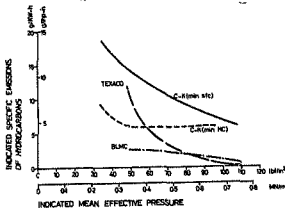


Figure B17 - Variation of HC emissions with indicated load

Operation at AFR's as lean as 50:1 overall demands that high swirl be induced during the second phase of combustion. This was achieved by an angled ICC port (Figure B13). The effect of changing this port configuration was monitored by measuring the transient pressures in each cylinder and by noting the pressure differences and the onset of knock.

Arques (16) comments, "The cycle and the engine conceived by Kouchoul presents the particular feature of enabling technical separation of the two functions of mass transfer and energy release during combustion". He presents a theoretical model of the C-K engine and concludes that the engine is well adapted to the study of flame propagation in SI engines.

B.3 Specific Areas of Study

Presented here are areas of engine design which effect LB engine performance and emissions. Certain of these may be incorporated into the research engine by future researchers.

The material is discussed under the following headings:

- B.3.1 Ignition systems
- B.3.2 Orifice and prechamber size and shape
- B.3.3 External devices (eg catalytic converters)
- B.3.4 Combustion chamber size and shape
- B.3.5 Fully open air throttling

B.3.1 Ignition systems

Tanuma et al (17) studied the effects of spark plug gap width, gap projection, spark energy, and mixture turbulence on the lean limit of their research engine. They found that:

1. The lean limit is highest and least effected by spark gap width with small centre electrode diameters (Figures B18, B19, B20)

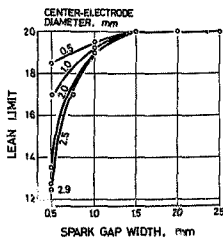


Figure B18 - Effect of gap width and centre electrode diameter on lean limit

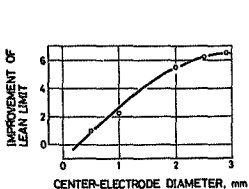


Figure B19 - Improvement of lean limit by widening gap width from 0,5 mm to 1,0 mm

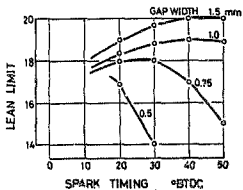


Figure B20 - Effect of gap width and spark timing on the lean limit

2. The lean limit extended the highest AFR with the deepest spark plug gap projection into the cylinders (Figure B21).

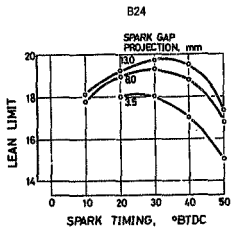


Figure B21 - Effect of spark plug gap projection on lean limit

3. Varying the spark energy at constant ignition timing did not extend the lean limit significantly. The greatest effect occurred at the lower spark plug gap widths (Figure B22).

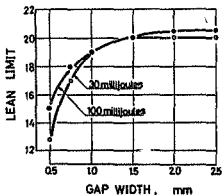


Figure B22 - Effect of spark energy on lean limits

4. Increasing the inlet mixture turbulence using shrouded inlet valve guides improved the lean limit and $sm\dot{v}$ of operation considerably on their engine.

Dale and Oppenheim (18) review the more novel methods of ignition for lean burn engines:

1. High energy spark plugs
2. Plasma jet igniters
3. Photochemical, laser and microwave ignition concepts
4. Torch cells (pre-chamber cavities)
5. Divided chamber SC engines (pre-chamber with separate inlet)
6. Flame torch igniters (as 5 but using small orifices)
7. Combustion jet igniters (as 6 but supersonic torch velocities)
8. EGR (exhaust gas recycling) ignition systems

They conclude that on the basis of fast dispersion of ignition sources to improve LB operation, the EGR, combustion jet and plasma jet igniter systems are the most desirable. Such systems are still under research and no production examples exist.

Oblander et al (19) tested an engine fitted with two, rather than a single spark plug per cylinder (Figure B23). While the technique led to still unacceptable emission characteristics, it did verify the faster rates of pressure rise and the increase in the lean limit.

B25

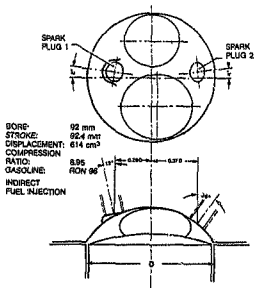


Figure B23 - Combustion chamber design of single cylinder engine with dual ignition

B.3.2 Orifice and pre-combustion chamber size and shape

Sinnanon and Cole (20), using a modified Cooperative Fuel Research (CFR) flat head engine with a divided chamber head, studied the effects of varying the pre-chamber and main chamber inlet AFR's. They defined the term 'degree of stratification' as the ratio of prechamber to main chamber equivalence ratios at ignition. Both chambers were fitted with their own inlet systems (Figure B24).

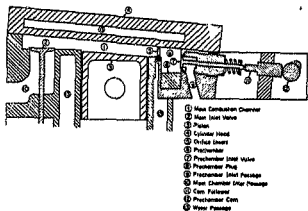


Figure B24 - Cross section of CFR engine

Although the prechamber on the research engine tested by the author is itself a cylinder (the mixture cylinder) which is used to extract power, the following finding of the above study may be of relevance:

1. The shape and cross-sectional area of the connecting orifice affects the intensity of combustion induced turbulence, produced by the torch jet.
2. The relative size of the rich and lean zones can be controlled by the choice of prechamber and main chamber volumes.
3. The best fuel consumption occurred with an overall equivalence ratio of 0.8. The least variation in fuel consumption over a wide range of overall mixtures occurred with the lowest degree of stratification (Figure B25).

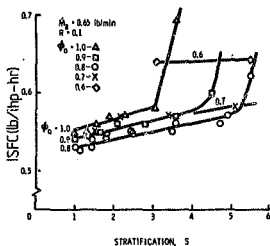


Figure B25 - Effect of stratification and overall equivalence ratio on fuel consumption

Yagi et al (21) observe that a branched conduit type torch passage between the auxiliary and main combustion chambers results in improved anti-knock qualities (Figure B26).

It has been confirmed by high speed photography (22) that the different pressure drops across each conduit results in one branch igniting the main charge only. The pressure rise in the main chamber recirculates the unburnt gases in the remaining conduits. Figure B27 demonstrates the anti-knock improvements at full throttle on the engine used by Yagi et al. The compression ratio was 8.8:1 and $\Delta\theta$ is the difference between the crank angle at the onset of knock and the minimum best torque advance (NBT).

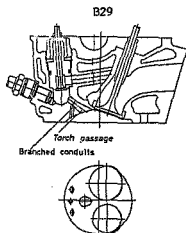


Figure B26 - Branched conduit type of combustion chamber

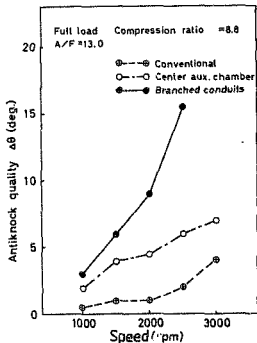


Figure B27 - Anti-knock quality of stratified charge engines

Although fuel injection into both the auxiliary and main chambers was used, Kataoka and Hirako (23) observed the importance of the torch issuing from the orifice. A well regulated torch caused a rapid

combustion even with a fairly lean mixture (Figure B28). This occurs since, as the orifice diameter is decreased, a larger fraction of the mixture is burnt in the early stage, *reducing* the combustion duration and consequently a higher peak pressure can be obtained in the cycle (Figure B29). This indicates that the combustion process is related to the torch kinetic energy.

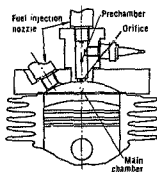


Figure B28 - Cross section of combustion chamber

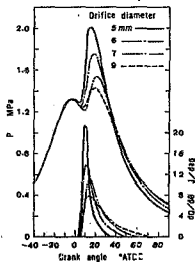


Figure B29 - Effects of orifice dimensions

B.3.3 External devices

Goulburn and Hughes (24) presented a study of the homogenization of the inlet air-fuel mixture by means of heating. The advantages of the leaner mixtures, namely improved thermal efficiencies and emission characteristics offset the reduction in volumetric efficiency.

B.3.4 Combustion chamber size and shape

Lucas and Brunt (25) investigated the interaction of combustion chamber shape, spark plug location and compression ratio. Designs tested were the May Fireball, 'bathtub' and 'disc'.

They conclude that for fixed compression ratios, flame speed is not effected by combustion chamber shape but the rate of combustion pressure-rise and cyclic dispersion are. Thus, for lean mixtures, combustion chambers capable of fast combustion rates are preferred. Examples include the 'bowl-in-piston' and May Fireball designs.

B.3.5 Fully open air throttling

The elimination of inlet air throttling, and the control of power by means of fuel supply only, results in a charge of higher density and thus an improved volumetric efficiency. Harrow and Clark (26) studied such operation on an LB engine. A mixture generator provided a homogeneous inlet charge. The following tests were conducted:

1. A wide open throttle (WOT) the AFR was varied and spark plug timing optimised to MBT.
2. At WOT the spark timing was varied at various AFR's until knock occurred.

3. For a series of AFR's, the engine was throttled and spark timing optimized.

It was concluded that with normal carburation (ie in the absence of a mixture generator, such operation would cause a complex pattern of instability, and even with a mixture generator a WOT condition could be used only at the top 30% of the indicated power output. Also, the advance in microprocessor technology could allow automatic advances in spark timing.

B.4 Miscellaneous

Sakai et al (27) and Hall and Sorenson (28) compared the performance of a conventional engine with that of the same engine modified for LB operation. In both studies LB operation led to lower CO and NO_x and higher HC emissions. No noticeable improvement in fuel consumption occurred when converting to LB operation.

APPENDIX C**DESCRIPTION OF THE RESEARCH ENGINE**

The mode of operation and a brief description of the research engine was presented in Appendix A, p A7. Mechanical details and history of modification to the engine follow.

C.1 Basic Engine Dimensions

The research engine is a modified version of the Yamaha 55BM, an outboard engine for marine applications. This is a two-cylinder, normally aspirated (two carburetors), two-stroke engine having a rated maximum power of 40 kW (55 HP). Typical of two-stroke cycle engines, peak power is developed at high speeds namely 7000 rev/min (Figure C1).

The first cylinder leads the second by a crankangle of 180° , with piston strokes of 72 mm. Each cylinder has a bore of 82 mm, giving an over-square engine of 760 cm^3 capacity. The carburetors are located on the crankcase, the mixture being contained by the usual reed valve arrangement. Combustible mixtures are supplied to the cylinders via three transfer ports per cylinder.

A scaled tracing of the cross-section of the cylinder ports are shown in Figure C2. The approximate areas of the exhaust port and each transfer port are 1460 mm^2 and 470 mm^2 respectively. The top of each piston at the circumference coincides with the top of each cylinder sleeve. Thus the top of the sleeve was used as the datum for the relationship between piston depth and crank angle (Table C1, Figure C3).

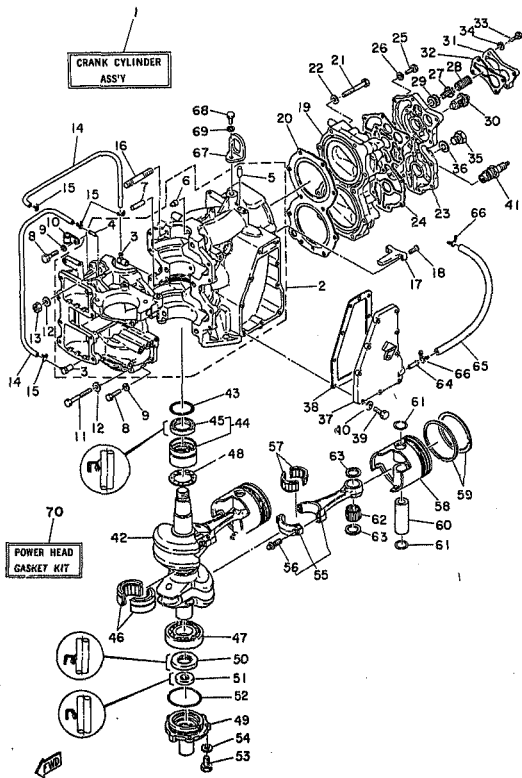


Figure C2 - Production Yamaha 558M engine

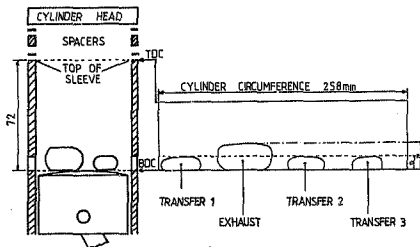


Figure C2 - Cylinder port location and dimensions

TABLE C1 - Piston depth (below cylinder sleeve) vs crank angle

Piston depth (mm)	Crank angle(Deg)	Piston Depth (mm)	Crank angle (Deg)	Piston Depth (mm)	Crank Angle (Deg)
0	0 (TDC)	62,8	130		
0	10	64,7	135	52,9	250
2,4	20	66,3	140	48,4	260
7,0	30	68,7	150	41,3	270
10,7	40	70,5	160	34,5	280
15,4	45	71,6	170	28,1	290
17,3	50	71,9	180 (BDC)	21,5	300 ¹
23,9	60	71,6	190	15,3	310
28,9	70	70,4	200	12,5	315
36,6	80	68,5	210	10,0	320
42,7	90	65,8	220	5,7	330
48,7	100	64,2	225	2,5	340
54,2	110	62,2	230	0,5	350
58,9	120	58,0	240	0,1	360 (TDC)

Figure C3 - Piston depth vs crank angle

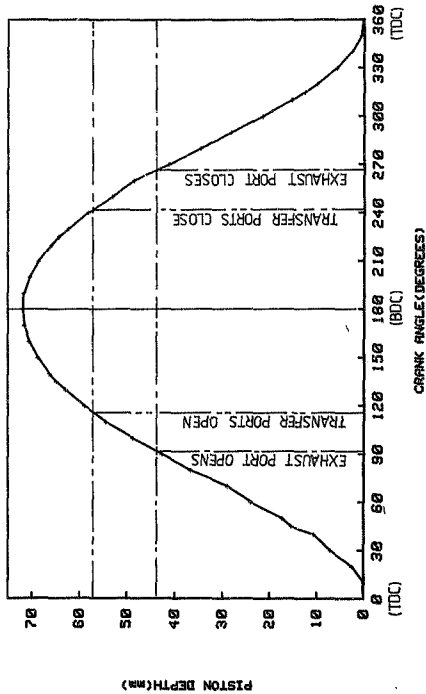


Figure C4 shows the range of crank angles for which the exhaust and transfer ports are open. This information will be of use when studying the cylinder combustion pressure curves. The exhaust port is open between 92° and 266° after TDC. The transfer ports are open between 115° and 244° after TDC.

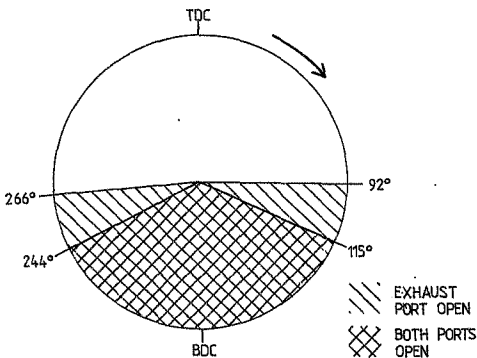


Figure C4 - Port timing on research engine

C.2 Engine Modifications by Past Researchers

The engine as supplied by Mr R M Amm was fitted with his patented cylinder head of variable compression ratio stratified charge design (VCRSC). The crankshaft had been rebuilt so that both pistons moved in unison. This modification was necessary both for the VCRSC cylinder head and for the head tested in this study.

O'Brien and Ne1 (29), during their final year research project in 1984 initiated the conversion of the engine and test rig to its present form. In order to connect the engine to a water brake dynamometer, the crank flywheel was removed. The flywheel also contained part of the ignition system. Details and drawings of all modifications and equipment acquired are presented in their report (29).

A new flywheel was manufactured to be used for starting the engine manually with a ripcord. The redesigned ignition system was fitted to the final drive end of the crankshaft, and utilized a standard breaker-point and cam system with no automatic advance. Manual adjustment of the ignition timing during engine testing was considered important and allowed for.

A new single piece aluminium cylinder head (Figure C5) was manufactured which uses the existing water cooling system of the engine. The resulting combustion chambers are of the disc type with centrally located spark plugs. Provision for the fitting of pressure transducers was made (Figure C5). The inter-cylinder transfer port is wide but shallow (40 x 2mm), the cross-sectional area having been selected on the basis of the work of Hirako and Kataoka (23). The port was not machined at an angle to the line connecting the centres of the cylinder bores, as practiced with the Cranfield-Kushul engine, since the direction of swirl in the cylinders for the Yamaha was not known. The cooling jacket may also be seen in Figure C5.

A spacer plate and two gaskets nest between the cylinder sleeves and the head to reduce the compression ratio (Figure C5).

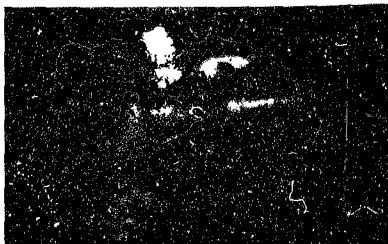


Figure C5 - Cylinder head and water cooling jacket

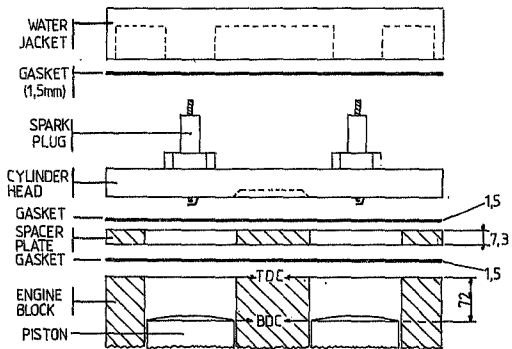


Figure C6 - Cylinder head assembly

Using Figure C6, (and neglecting the volume of the inter-cylinder connecting port), the nominal and effective compression ratios were calculated as follows:

Nominal compression ratio

At BDC $V_1 = 2 \times \pi/4 * d^2 * S_1$ where: $d = 82 \text{ mm}$
 $S_1 = 82,3 \text{ mm}$

$$V_1 = 8,653 \times 10^{-6} \text{ m}^3$$

At TDC $V_2 = 2 * \pi/4 * d^2 * S_2$ where: $d = 82 \text{ mm}$
 $S_2 = 10,3 \text{ mm}$

$$V_2 = 1,0879 \times 10^{-6} \text{ m}^3$$

Volume compression ratio = CR = V_1/V_2

$$\text{CR} = 9/1$$

Nominal CR 8:1

Effective compression ratio

As the pistons close the exhaust port

$V_1 = 2 \times \pi/4 * d^2 * S_1$ where: $d = 82 \text{ mm}$
 $S_1 = 82,3 - 28 = 54,3 \text{ mm}$

$$V_1 = 5,735 \times 10^{-6} \text{ m}^3$$

At TDC $V_2 = 1,0879 \times 10^{-6} \text{ m}^3$ as previously

Effective CR 5,3 : 1

Originally the research engine ran with the crankshaft axis vertical, as intended by the manufacturers. The intake manifold had to be replaced with one that allowed the carburetors to operate with the engine mounted horizontally. Both carburetors were connected to a common air reservoir. The air flow into the reservoir was measured using an orifice plate with corner tappings.

The research engine was never run by Nel and O'Brien, hence no test results using the new cylinder head were available.

C.3 Further Modifications During the Present Study

In order to permit reliable operation of the test facility, a number of further modifications had to be made to the engine, the dynamometer and the coupling between the two. Details of yet further modifications permitting the installation of instrumentation are discussed in the following Appendix.

The engine could not be started manually using the rickcord. An electric motor was thus used as a starter (Figure C7). By means of flat belt pulleys fitted to the motor and dynamometer, (203 and 406 mm diameter respectively), the research engine was motored at 860 rev/min via the dynamometer. The ignition was then switched on, and once the engine had started, power to the electric motor was disconnected. If desired, the belt could be removed by pivoting the motor base plate fully upwards. A guard was fitted around the dynamometer pulley.

In addition to ease of starting, the ability to motor the engine proved most useful in the calibration of instruments and the alignment of the engine and dynamometer.

C10

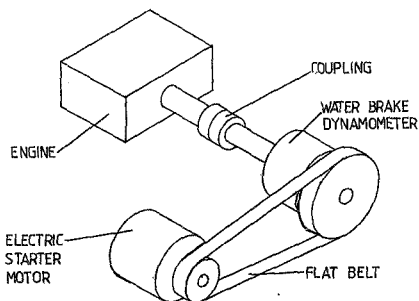


Figure C7 - Starter motor assembly

Only one common air inlet reservoir to both carburetors was fitted. Hence air inlet pressures could be equalised only by varying the throttle settings. In order to permit testing under a wider range of conditions, and to investigate the use of no air throttling on one cylinder, the dependence of fuel flow on the air throttle setting (as in conventionally aspirated engines) was removed. This was achieved by modifying the carburetors and fitting an externally adjustable needle directed into the main fuel jet within each carburettor. It was now possible to vary the air fuel ratio into each carburettor without changing the main jet (Figures C8-C11).

Lubricant for this 2-stroke engine was premixed into the fuel. Consequently, leaning out the air-fuel mixture in the lean/air cylinder would also decrease the quantity of lubricant and increase the possibility of seizure.

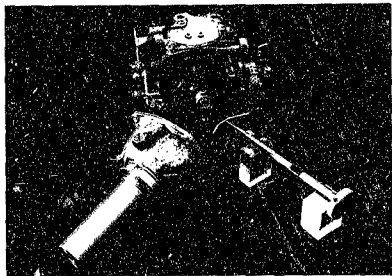


Figure C8 - Fuel flow throttling device

To overcome the above danger in lean burn operations, an auxiliary lubrication system was provided as a supplement. The lubricant was induced into the vacuum between the air cylinder carburettor and the reed valve (Figure C12). A needle valve permitted equalization of the lubricant flow rate under varying vacuum pressures.

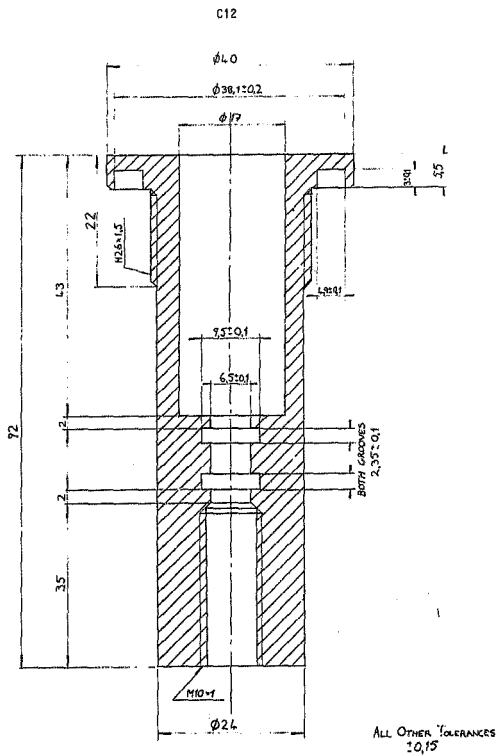


Figure C9 - Needle housing

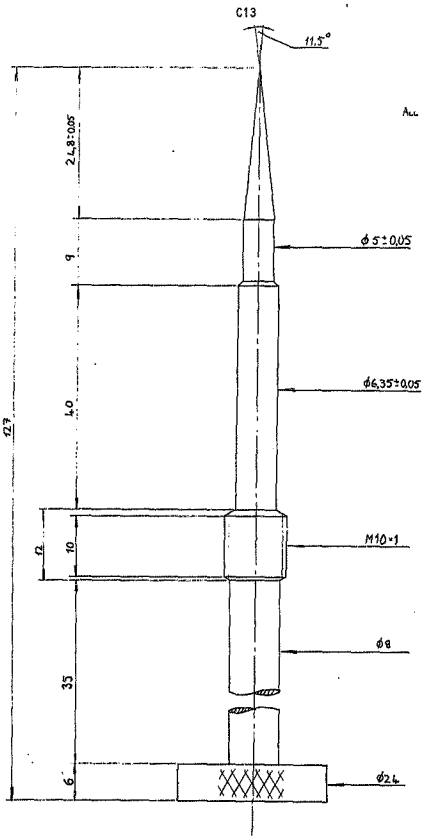


Figure C10 - Fuel needle

C14

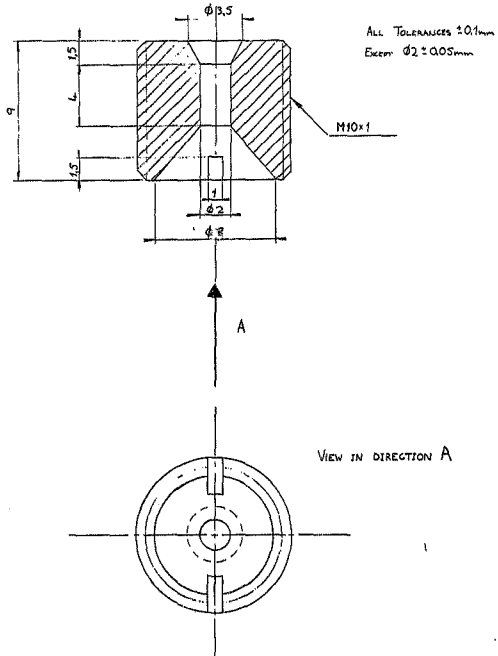


Figure C11 - Main fuel jet

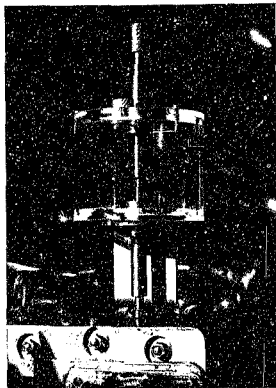


FIGURE C12 - Air cylinder lubricant reserve

In order to improve the low fuel line pressures, a Mitsuba diaphragm electric fuel pump was installed into each fuel line. The fuel pumps also contained filters which could not be installed previously due to the increased fuel line losses.

During preliminary testing, the research engine and dynamometer were found to be misaligned. Also, the coupling (Fenner HRC 130) had been eccentrically machined. The total result of these errors was a vibration

C16

during running of approximately three millimetres amplitude. This was originally thought to be due to the inherent lack of primary imbalance in the research engine.

After remachining the couplings and realigning the engine and dynamometer, the engine was secured to the base plate and located using dowel pins.

Henceforth, should the coupling require any maintenance, the dynamometer half may be slid back, the flexible water cooling pipes removed, the air intake reservoir disconnected, and the engine loosened and removed. Replacing the engine to the base plate and refitting the dowel pins, will ensure that the engine and dynamometer will be immediately realigned. Thus, it is not recommended that either the dynamometer or the engine base plate be moved from their present location.

APPENDIX D

INSTRUMENTATION

This appendix describes the instrumentation system used in determining engine performance characteristics. The emission of pollutants was not monitored.

D.1 Test System Parameters

The interrelation between operator induced input parameters, inherent engine parameters and engine output parameters is shown in Figure D1.

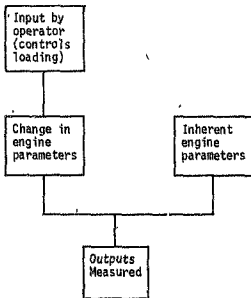


Figure D1 - Logic diagram of engine inputs and outputs

D.1.1 System inputs

The input parameters which were varied by the operator during this study were the engine loading, fuel and air flow rates to the cylinders, and the spark ignition timing.

D.1.2 System outputs

The parameters which were measured during testing, and the type of instrumentation fitted to the system are discussed below.

Combustion chamber pressures

The transient pressure in both combustion chambers was monitored in order to observe the onset of knock and to ascertain the direction of charge transfer through the inter-cylinder transfer port. Piezo-electric pressure transducers are best suited to this task.

Fuel consumption

The fuel supply to each cylinder was independently measured using constant volume glass fuel flow meters. In view of the large variation in fuel flows (while leaning out the air cylinder), neither rotameters nor turbine bladed fuel flow meters were considered suitable. At a later stage positive displacement gear pump fuel flow meters with an analogue output were fitted, in order to reduce the time taken for each test, and to provide a means of continuously monitoring the fuel flow rate to each cylinder.

Speed

Engine speed was measured using a digital hand-held tachometer.

Torque

The engine's power output was absorbed using a water-brake dynamometer. The torque could be read off a dial connected to the pivoting dynamometer housing.

Air mass flow rate

The total air flow rate to this engine was measured using an orifice plate fitted to the inlet of an air surge damper drum. At present, a common drum supplies air to both mixture and air cylinders, thus limiting testing to equal air throttle settings (that is, equal air mass flow rates to both cylinders).

Inlet air temperature

The inlet air temperature was measured by a thermocouple fitted to the interior of the surge drum.

Exhaust gas pressure

Some means of recording combustion pressure with respect to atmospheric pressure was required. Hence a manometer was fitted to the exhaust manifold from which the mean exhaust pressure was read. This exhaust pressure was taken to coincide with the minimum combustion chamber pressure recorded after the exhaust port had opened (EPO) (Figure D2).

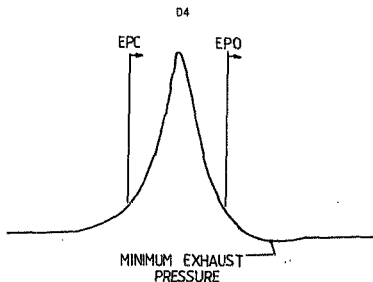


Figure D2 - Exhaust pressure datum

Transfer port differential pressures

It was found that it was not possible to balance the carburetors during testing; thus the pressures across the transfer ports were balanced instead. This was achieved by tapping holes into one of each cylinder's transfer port and connecting a differential piezo-electric transducer across them.

D.2 Specification and Calibration of Instruments

D.2.1 Combustion chamber pressures

Instrument description : Piezo-electric pressure transducers
 Make : Kistler
 Origin : Winterthur, Switzerland
 Model : 6121A1
 Application : One fitted per cylinder enclosed in a protective water cooled jacket (Figure D3)

Serial number : 143266 (mixture cylinder)
 : 179756 (air cylinder)
 Range : 0-250 bar
 Sensitivity : -13.95 pV/bar (mixture cylinder)
 : -12.9 pC/bar (air cylinder)
 Output to : Kistler charge amplifiers, model 5001
 Calibration : Supplied with instrument by manufacturers

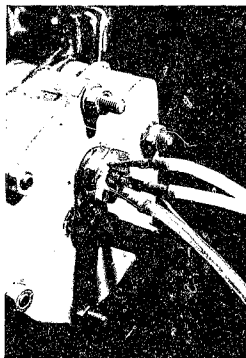
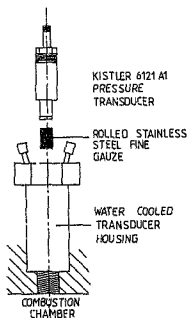


Figure D3 - Water cooled transducer housing - disassembled and assembled into cylinder head with transducer

D.2.2 Fuel consumption

Two methods of fuel consumption were used during testing.

- 1) Instrument description : Glass bowl fuel flow meters. One bowl per fuel supply line to each cylinder. The time taken for each bowl to empty was recorded.
- Make : Manufactured in-house
- Application : Fitted between the main fuel supply tank and each cylinders carburettor. (Figure D4)

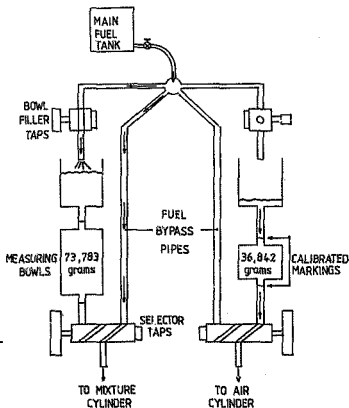


Figure D4 - Glass bowl fuel flow meters

Bowl specifications : 73,783 g fuel (mixture cylinder)
 36,842 g fuel (air cylinder)
 Calibration : see Table D1

Table D1 Calibration of glass bowl fuel flow meters

BOWL	Test 1 (g)	Test 2 (g)	Test 3 (g)	Mean (g)	Standard deviation (g)
Mixture cylinder	73,80	73,85	73,70	73,78	0,0624
Air cylinder	37,00	36,75	36,77	36,84	0,0471

1) **Instrument description** : Positive displacement gear pump fuel flow meter with continuous analogue display and voltage output

Make : Pierburg
Origin : Neuss, West Germany
Model : PLU 106
Application : One fitted per cylinder between the main fuel supply tank and each cylinder carburettor (Figure D5)
Serial number : 3749 (mixture cylinder)
 : 2542 (air cylinder)
Calibration : The indicated outputs both from the analogue display and the DC voltage output were recorded for a variety of fuel flows. The fuel flows were obtained by throttling the output of each fuel pump and measuring the rate of change of mass as the fuel was discharged into a beaker on an electronic balance.

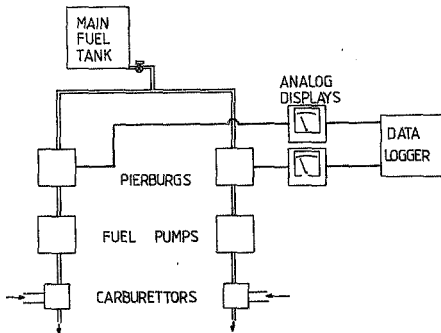


Figure D5 - Pierburg fuel flow meters in fuel supply line

Table D2 Pierburg 3749 fuel flow meter calibration - Mixture cylinder

Display output (l/hr)	Electrical output (mV)	Fuel mass change (g)	Time (s)	Fuel flow Rate (g/s)
0,85	11,4	36,0	221	0,163
1,10	14,2	36,0	185	0,195
1,75	22,0	36,0	107	0,336
2,80	35,3	46,0	84	0,548
3,60	45,6	80,0	85	0,706
4,05	51,7	85,0	105	0,810
4,92	62,5	85,0	89	0,960

PIERBURG SN:3749 RIGHT CYLINDER

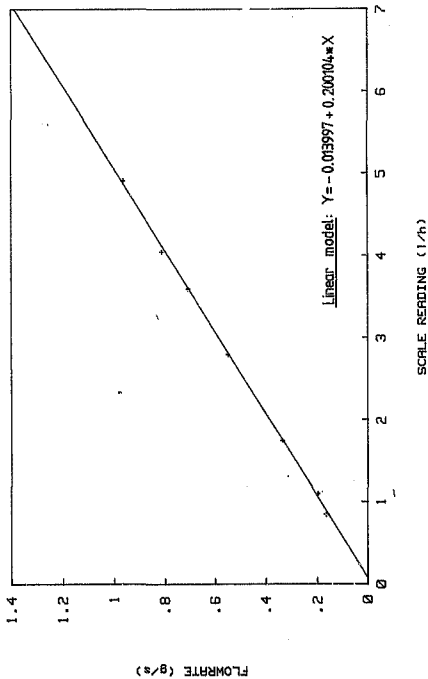


Figure D6 - Calibration: Pierburg 3749 fuel flow meter

Table D3 Pterburg 2542 fuel flow meter calibration - Air cylinder

Display output (l/hr)	Electrical output (mV)	Fuel mass Change (g)	Time (s)	Fuel Flow Rate (g/s)
1,50	6,9	20,0	59,4	0,337
1,80	8,1	25,0	64,2	0,389
2,00	9,1	25,0	58,2	0,430
2,70	12,2	35,0	60,4	0,579
3,55	15,8	45,0	59,2	0,760
4,20	18,9	55,0	61,0	0,902
4,60	20,6	60,0	61,8	0,971
5,10	22,3	65,1	61,2	1,064
6,20	27,2	80,3	62,0	1,295

PIERBURG SN:2542 LEFT CYLINDER

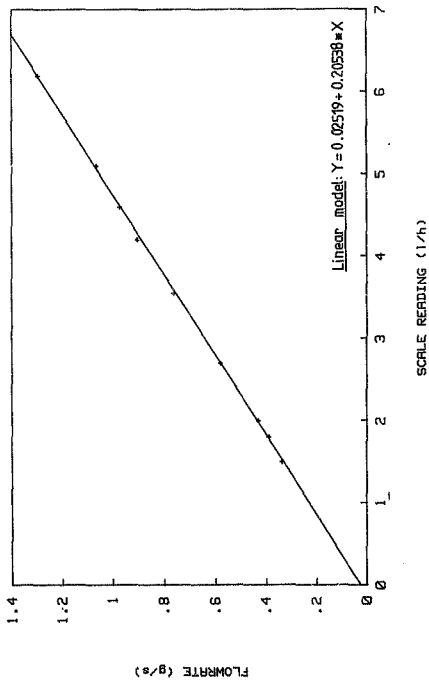


Figure D7 - Calibration: Pierburg 2542 fuel flow meter

D.2.3 Torque

Instrument description : Water brake dynamometer with mechanical analogue torque output indicator

Make : Hoffmann

Origin : Eira, West Germany

Model : Not known

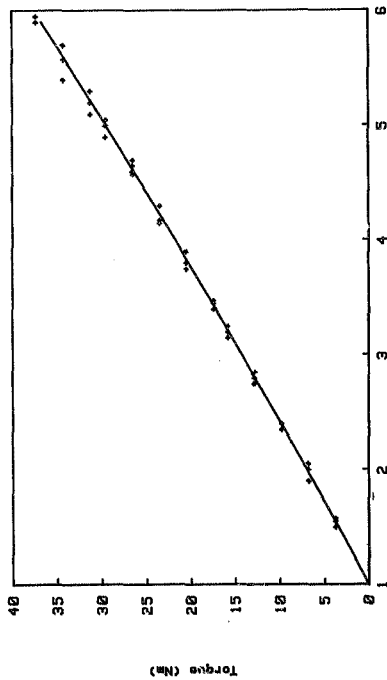
Application : Driven from engine via Fenner HRC 130 coupling

Calibration : Applying torque to the dynamometer statically using known masses and a lever arm (Table D4, Figure D8). Engine vibration was simulated by lightly tapping the dial face.

Table D4 Dynamometer calibration

Test No	Applied torque (Nm)	Indicated output (units)	Test No	Applied torque (Nm)	Indicated output (units)
1	0	1,025	15	37,30	5,950
2	3,73	1,500	16	34,28	5,706
3	6,78	1,900	17	31,23	5,300
4	9,80	2,350	18	29,53	5,000
5	12,77	2,750	19	26,49	4,650
6	15,81	3,150	20	23,47	4,300
7	17,45	3,400	21	20,49	3,900
8	20,49	3,800	22	17,45	3,475
9	23,47	4,175	23	15,81	3,250
10	26,49	4,575	24	12,77	2,850
11	29,53	5,000	25	9,80	2,350
12	31,21	5,200	26	6,78	2,050
13	34,28	5,575	27	37,33	4,575
14	37,30	5,950			

Dynamometer Calibration



Gauge Reading

FIGURE D8 - Dynamometer calibration

D.2.4 Mass flow rate of air

Instrument description: Orifice plate fitted to inlet of air surge damper drum with corner tappings. Manufactured according to ISO 5167-1980(E).

Remarks : Three orifice plates were available (as required) having diameters of 20,0, 25,0 and 35,0 mm respectively. The 20,0 mm orifice plate was used for testing.

Orifice plate calculation : Preliminary tests for the speed ranges required showed the 20 mm orifice plate to be suitable - the criteria being that the pressure drop should never exceed 200 mm of water, this value being the maximum of a range on the digital electronic AIR (Air Instruments Resources) micromanometer used (Model MP5KMD)

$$\dot{q}_m = \alpha \cdot E \cdot \frac{\pi}{4} \cdot d^3 \cdot \sqrt{2 \Delta p \rho_f}$$

where : \dot{q}_m = mass flow rate (kg/s)
 d = orifice diameter = 0,02 m
 ρ_f = atmospheric air density (kg/m³)
 Δp = change in pressure (Pa)
 α = flow coefficient
 E = expansion factor
 D = diameter of reservoir $\approx 0,6$ m
 C = coefficient of discharge = $\frac{\alpha}{E}$
 E = velocity of approach factor ≈ 1

$$\beta = \frac{d}{D} \approx 0 \text{ thus } C = 0,5959$$

$$\alpha = CE \text{ thus } \alpha \approx C = 0,5959$$

$E \approx 1$ for assumed incompressible fluids

$$\Delta p = \rho \cdot g \cdot \Delta h$$

where : ρ = density of water ≈ 1000 kg/m³
 g = 9,79546 m/s²
 Δh = drop across orifice (m H₂O)

$$\Delta P[\text{Pa}] = 1000 \left[\frac{\text{kg}}{\text{m}^3} \right] \cdot 9,79546 \left[\frac{\text{m}}{\text{s}^2} \right] \cdot 0,001 \cdot \Delta h [\text{mm}]$$

$$1000 \Delta P [\text{kPa}] = 9,79546 * \Delta h [\text{mm}] - (1)$$

$$f_r = \frac{P}{R * T}$$

where : f_r = air density of atmosphere
 P = atmospheric pressure (Pa)
 R = 287 kJ/kg K
 T = temperature (K)

$$= \frac{P [\text{kPa}] * 1000}{287 * T} \quad \text{--- (2)}$$

Substituting (1) and (2):

$$\dot{q}_m = 0,5959 * \frac{\pi}{4} * 0,02^3 * \sqrt{Z * 9,79546 * \Delta h [\text{mm}] * \frac{P [\text{kPa}] * 1000}{287 * T [^{\circ}\text{K}]}}$$

$$\dot{q}_m = 1,5467 * 10^{-5} * \sqrt{\frac{P [\text{kPa}] * \Delta h [\text{mm}]}{T [^{\circ}\text{K}]}}$$

For all tests, air flow rate into each cylinder assumed equal. Thus

$$\dot{q}_{\text{mix}} = \dot{q}_{\text{air}} = \dot{q}_m / 2 = 7,73356 * 10^{-6} * \sqrt{\frac{P [\text{kPa}] * \Delta h [\text{mm}]}{T [^{\circ}\text{K}]}}$$

D.2.5 Inlet air temperature

Instrument description : Thermocouple Type J
Application : Fitted into air inlet tank
Output to : Fluke 2240A Datalogger . ch cold junction compensation to provide an output in degrees centigrade.

D.2.6 Exhaust pressure

Instrument description : Water manometer
Application : Fitted to exhaust manifold of engine to provide a differential pressure between the mean exhaust pressure and atmospheric.

D.2.7 Transfer port differential pressure

Instrument description : Differential piezo-electric pressure transducer
Make : Kistler
Origin : Winterthur, Switzerland
Model : 7251
Application : Fitted across one pair of transfer ports for purposes of balancing air flow rates into each cylinder. Protection in case of engine backfire provided by taps, which were only opened when the transfer port pressures were being balanced.
Serial number : 42036
Range : 0 - 1 bar
Sensitivity : 2480 pc/bar
Output to : Kistler charge amplifier model 5001.

D.3 Data Processing

In order to reduce the time required to collect all output data for each test, the test procedure was computerised. Previously, the combustion

chamber pressures were captured by means of a transient recorder and thus hard copied using an X-Y plotter. This procedure was time-consuming because all desired graphs had to be plotted before the commencement of the next test. In addition, the gathered data was lost once the test pressures were recorded. Monitoring of the plotter and manually writing in the scales and titles of each graph was tedious and prone to error during the excitement of testing.

Computerization required the installation of some additional equipment and its incorporation into the overall system. It is this and the actual computer program used which is discussed in this section.

D.3.1 Computerization requirements

Pressure-time traces of each combustion chamber, and the differential pressure between them, were required to be able to analyse any charge transfer across the inter-cylinder connecting port. A plot of the differential pressure (measured between one transfer port of each cylinder), and of the spark ignition with respect to TDC to enable accurate measurement of the ignition timing was also programmed. The additional equipment required on the engine was a trigger mechanism and a spark ignition sensor.

Trigger circuit

A transient data recorder requires a trigger to sample the inputs from the engine's instrumentation in finite steps. The TDC's of both pistons were used to trigger the recorder, since on motoring the engine with the electric starter, TDC's coincide accurately with that chamber's maximum pressure. The trigger circuit could be monitored using an oscilloscope and adjusted to coincide with the peak pressure very accurately.

A stainless steel disc with one slit cut in was mounted between the engine and the coupling (Figure D9). The circumference of the disc

rotated within an optical emitter sensor unit (Texas Instruments TIL-143). The voltage comparator circuit (Figure D10) registered an output of 5 volts continuously to the transient recorder until the slit of the disc passed between the pickup. The comparator then returned to a quiescent state of approximately 0,2 volts. The trigger circuit of the transient recorder sensed the drop in voltage, and recorded the incoming data after a predetermined number of step voltages.

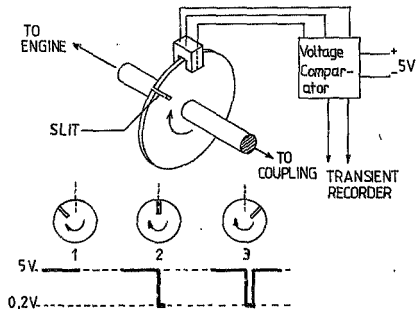


Figure D9 - Operation of TDC trigger circuit

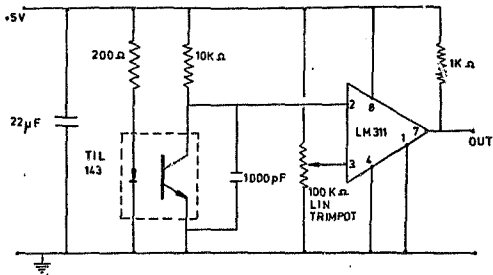


Figure D10 - Voltage comparator circuit

Ignition timing

The spark ignition was monitored by passing both spark plug leads through a current transformer, the output of which was transferred directly to the transient recorder.

D.3.2 Incorporation into instrumentation system

All outputs from the three charge amplifiers, as well as those from the TDC voltage comparator and the ignition timing current transformer, were fed to the transient recorder. When a test was conducted, the transient recorder, which had been continuously sampling the above data from the engine at a predetermined sample rate, was locked, and retained the last set of data stored. This information could thus be transferred to the computer and either stored on diskettes or plotted, using the computer program.

D.3.3 Computer program

The computer program was written in BASIC for the HP 9816 computer by N Lane and has formed the basis for most other engines tested in the Mechanical Engineering Laboratory. The program for the present tests, together with their results, are identified by the title 'YAMAHA'.

The first requirement for the program was to use the data stored in the transient recorder to produce scaled graphs of the following:

1. Pressure in the mixture cylinder vs time.
2. Pressure in the air cylinder vs time.
3. Superposition of the mixture and air cylinder pressures.
4. Difference between the mixture and air cylinder pressures.
5. Differential pressure across the transfer port of each cylinder.
6. Spark ignition trace.

All of the above were plotted with headings, axis scales and the TDC marker.

The second requirement (which was not used in the present study), was to process manually recorded data (for example, orifice pressure drop, fuel consumption in each cylinder, inlet air temperature, and engine torque and speed) to calculate air-fuel ratios, power, brake mean effective pressure and brake specific fuel consumption.

A flow chart of the program shows that each test is assigned a test code before the data is transferred onto disc (Figure D11).

D21

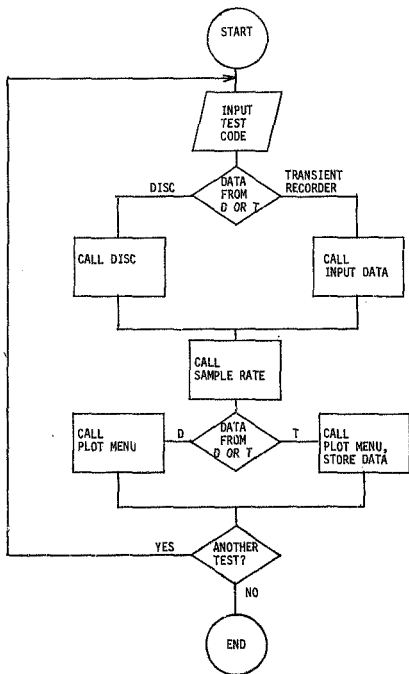


Figure D11 - Flowchart of computer program

APPENDIX E

RESULTS

E.1 Intended Test Procedure

Knowing that both carburettor air throttle settings had to be balanced for equal air mass flow, it was decided that the throttles be fixed for a series of tests (Figure E1). The loading and spark timing (adjusted for MBT) would be varied across as wide a speed range as possible. After completing a range of tests, the AFR on the air cylinder would be leaned out to another setting, and the procedure repeated.

The maximum safe running speed, considering the inherent lack of even primary reciprocating force balance in this engine was initially estimated to be no more than 3000 rev/min, while the minimum speed was found to be approximately 800 rev/min.

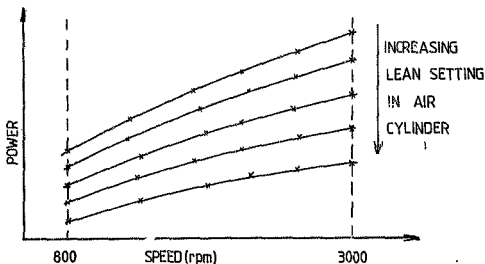


Figure E1 - Intended power-speed curves for one air throttle setting

The resultant power-speed graph would provide a useful means of monitoring the results during testing and selecting any trends in performance. Constant speed information could also be obtained (for example, MBT, spark timing, AFR, engine stability, engine knock, pressure differential across inter-cylinder connecting port).

The combustion chamber pressure curves would be useful to monitor:

1. The overall nature of combustion.
2. The onset of knock.
3. Significant changes in differential pressures of the combustion chambers.

E.2 Results Obtained

An initial test run (test code 1), with both fuel needles fully open, low engine loading (approximately 7 Nm) at speeds of 1210 rev/min, showed large combustion pressure fluctuations in both cylinders (Figures E2, E3). The mixture cylinder (cylinder 1) attained peak combustion pressures of over 27 bar, but these alternated with peak pressures of only 9 bar. The air cylinder (cylinder 2) behaved visually identically, but all peak pressures are lower by about 1 bar.

The exhaust pressure of the air cylinder rose throughout successive plotted cycles, as reflected in the trace of differential pressure across the inter-cylinder connecting port (Figure E4).

MBT was found not to be sensitive to spark timing. Figure E5 shows the spark timing to be 55° before TDC. Considering the low speeds and that the engine is a two-stroke engine, this value is extremely advanced. The shapes of all pressure curves however indicate that the spark timing was close to optimal and that no knock was observed.

CYLINDER 1 : 1

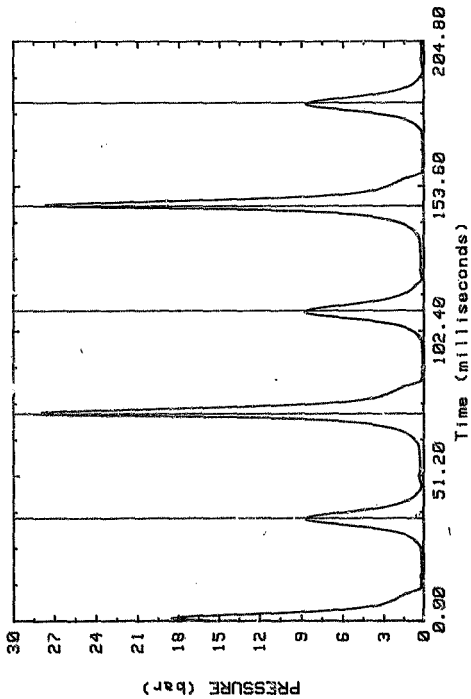


Figure E2 - Pressure trace - mixture cylinder: Test 1

CYLINDER 2 : 1

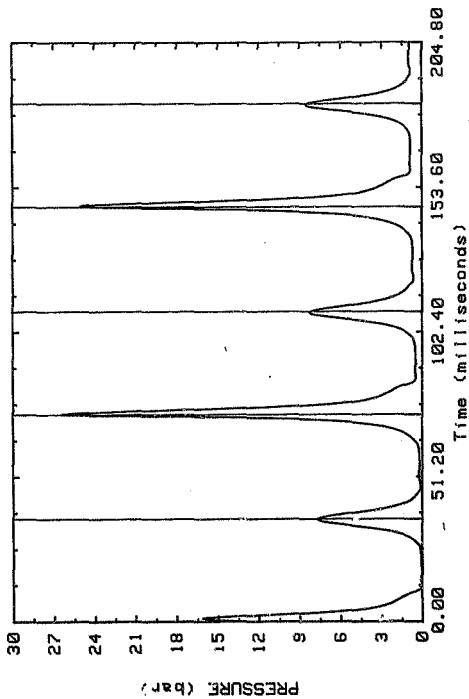


Figure E3 - Pressure trace - air cylinder: Test 1

CYLINDER 1 - CYLINDER 2 : 1

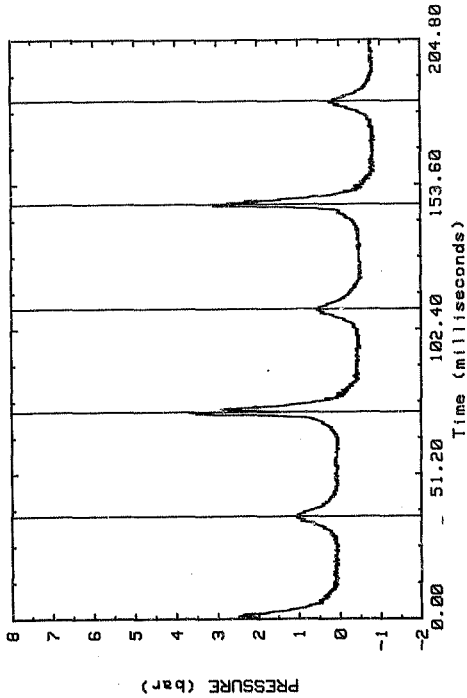


Figure E4 - Pressure trace - differential across cylinders: Test 1

SPARK TIMING : 1

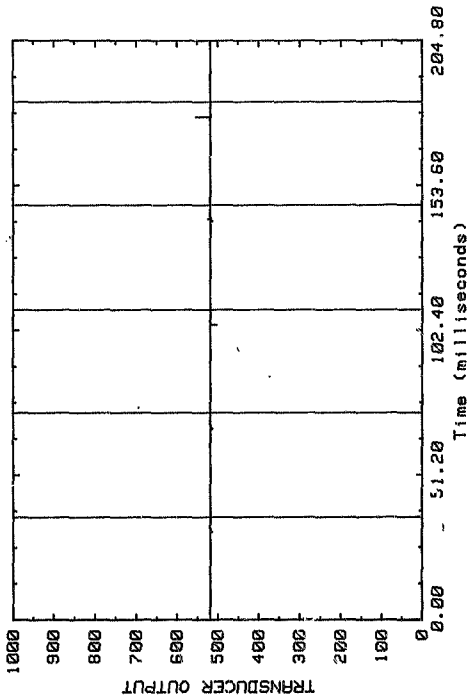


Figure E5 - Spark ignition timing: Test 1

During the following test session, the intended performance curves (as in Figure E1) were attempted. Three results (test code 09108501 to 09108503) were obtained before the coupling overheated (Table E1, Figures E6 - E20). For each test the loading was increased without varying the leanness of the air cylinder.

Table E1 - Test results, code 09108501 - 09108503

PARAMETERS	UNITS	TEST	TEST	TEST
		09108501	09108502	09108503
Speed	rpm	1680	1513	1485
Torque	Nm	2,30	3,65	8,60
Power	kW	0,405	0,578	1,337
Air fuel ratio - air cylinder (by mass)	-	2,94:1	3,43:1	3,47:1
Air fuel ratio - mixture cylinder (by mass)	-	6,62:1	7,90:1	7,90:1
Spark ignition timing	°Before TDC	48	40	22
Exhaust pressure	mm H ₂ O	110	130	220

Test code 09108501

Despite an advanced ignition timing of 48° before TDC, the pressure traces obtained for both cylinders show slight signs of late pressure rises for the high level pressure cycles (peak pressures approximately 20 bar). A power of 0,405 kW was developed with an overall AFR of 4,78:1. The exhaust pressure was very high (110 mm H₂O), which suggests a blockage in the exhaust passage.

CYLINDER 1 : 09108501

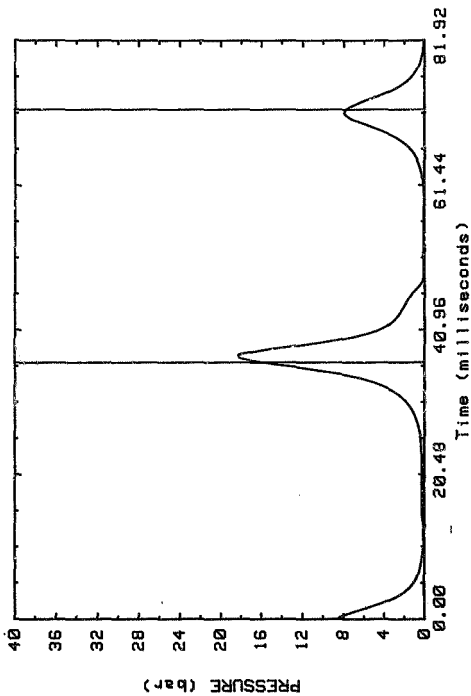


Figure E6 - Pressure trace - mixture cylinder: Test 09108501

CYLINDER 2 : 09108501

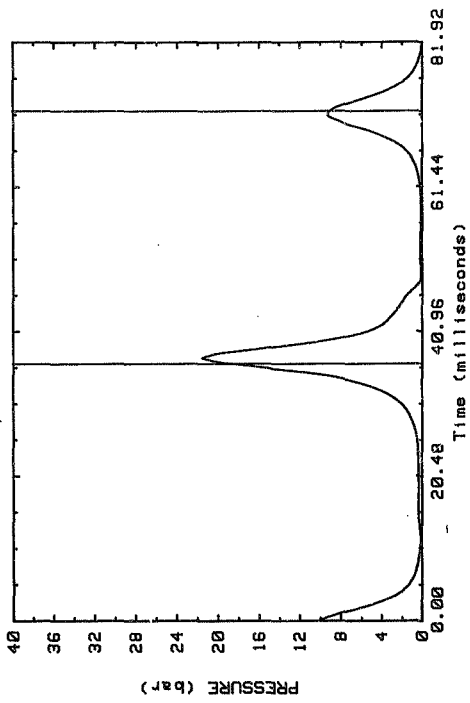


Figure E7 - Pressure trace - air cylinder: Test 09108501

CYLINDERS 1 & 2 : 09108501

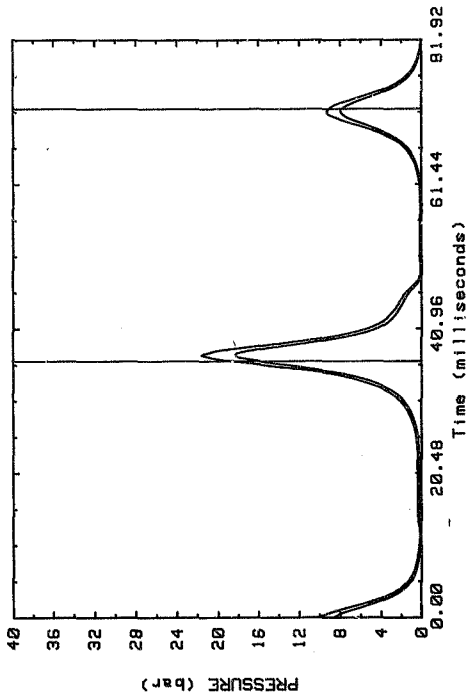


Figure E8 - Pressure trace - both cylinders: Test 09108501

CYLINDER 1 - CYLINDER 2 : 09108501

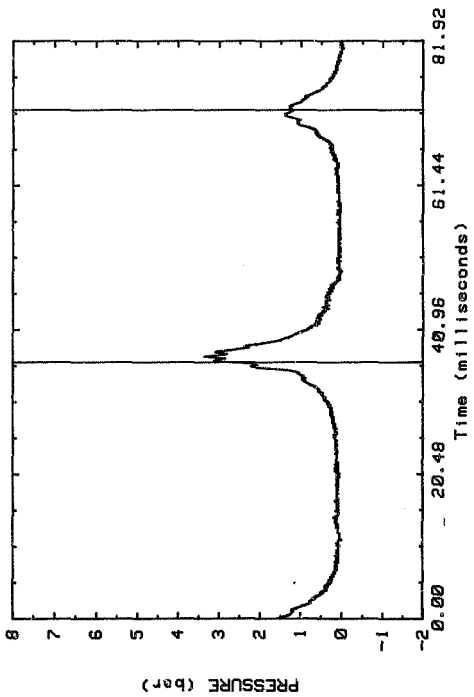


Figure E9 - Pressure tracé - differential across cylinders: Test 09108501

SPARK TIMING : 09108501

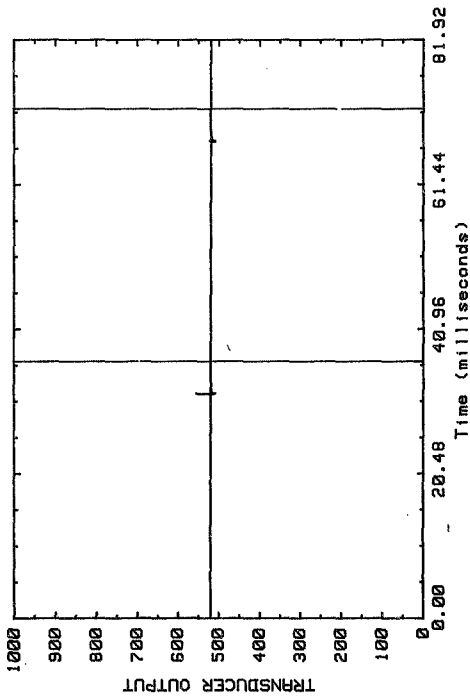


Figure E10 - Spark ignition timing: Test 09108501

Test code 09108502

This test differed from the previous one in that the power output was raised to 0,578 kW and the speed lowered to 1513 rev/min. A spark ignition timing of 40° before TDC, and an overall air fuel ratio of 5,67:1 improved the cyclic peak variation and the late pressure rise found in the previous test. The engine appeared to be running better, possibly owing to increased load.

Test code 09108503

On further increasing the engine load to 1,337 kW output at 1485 rev/min, the spark timing for MBT was found to be in the region of 22° before TDC. The overall AFR was 5,67:1, that is, similar to that of the previous test. The transient recorder sample rate had been increased to observe pressure variations over a greater number of cycles. Peak pressure variation between cycles was as high as 3 bar, although this did not often occur. The pressure difference between the cylinders remained reasonably constant at 1 bar (Figure E 19).

The next test at increased load did not succeed since the engine stalled. The spark timing was adjusted in an attempt to eliminate it, but to no avail.

The engine was next run starting with higher load (Test 09108504) and opening the air throttle wider. At an ignition timing of 39° before TDC, a speed of 1500 rev/min, and an indicated torque of 15 Nm, the pressure curves obtained in test 09108504 (Figures E21 to E25) were consistently low (approximately 10 bar). This pressure coincides with the pressure obtained when the engine was motored without ignition at 850 rev/min, suggesting lack of firing.

CYLINDER 1 : 09108502

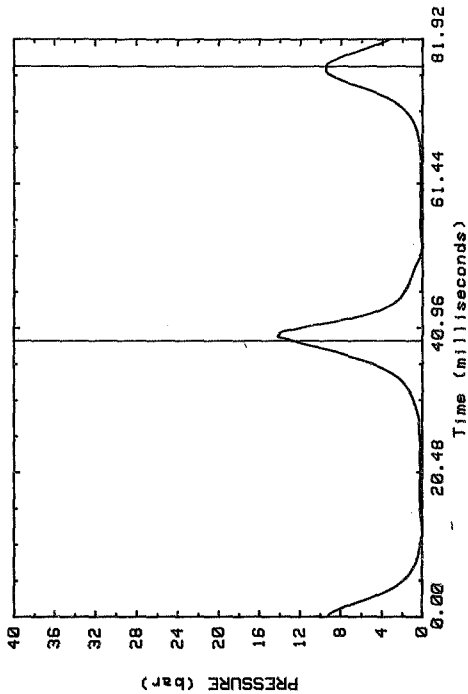


Figure E11 - Pressure trace - mixture cylinder: Test 09108502

CYLINDER 2 : 09108502

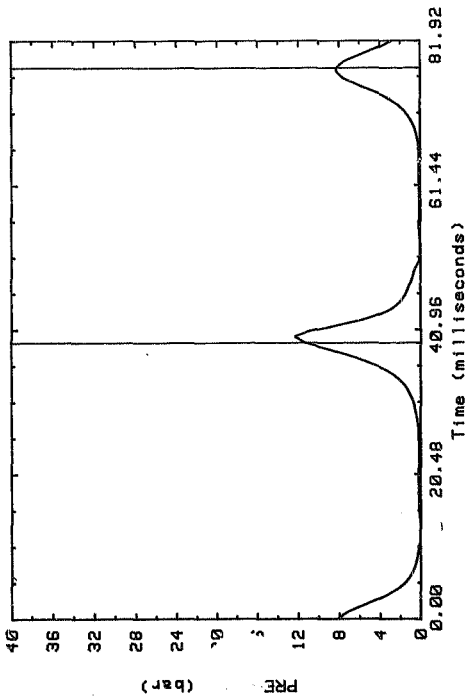


Figure E12 - Pressure trace - air cylinder: Test 09108502

E16

CYLINDERS 1 & 2 : 09108502

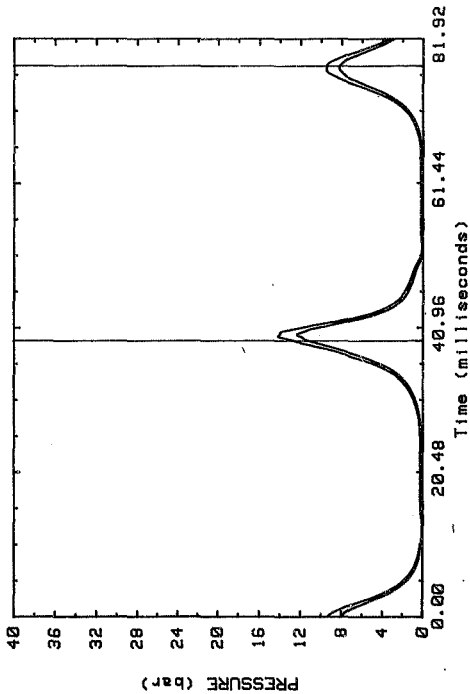


Figure E13 - Pressure trace - both cylinders: Test 09108502

CYLINDER 1 - CYLINDER 2 : 09108502

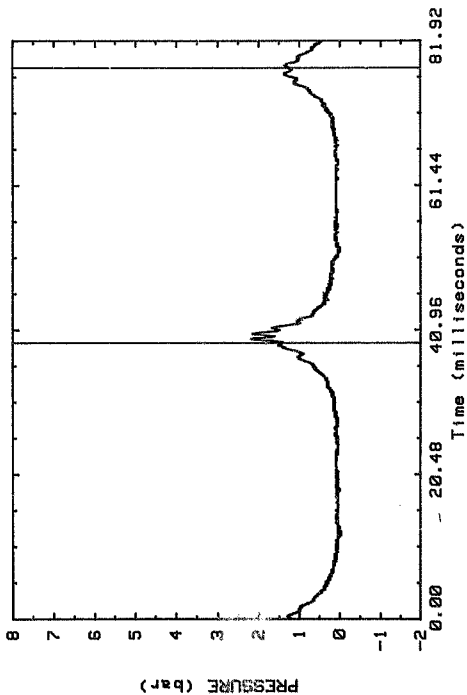


Figure E14 - Pressure trace - differential across cylinders: Test 09108502

SPARK TIMING : 09108502

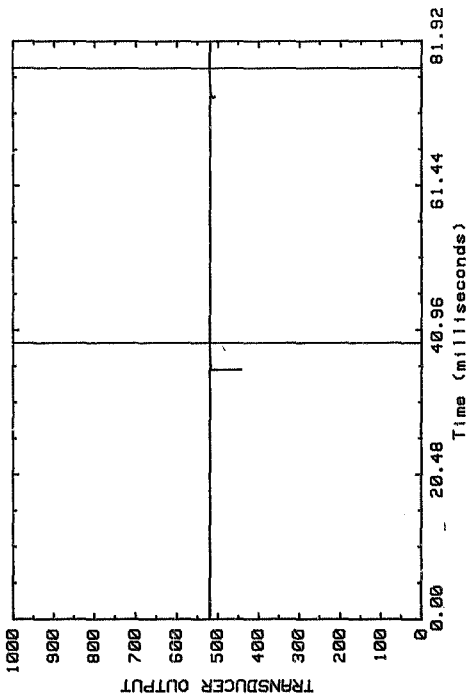


Figure E15 - Spark ignition timing: Test 09108502

CYLINDER 1 : 09108503

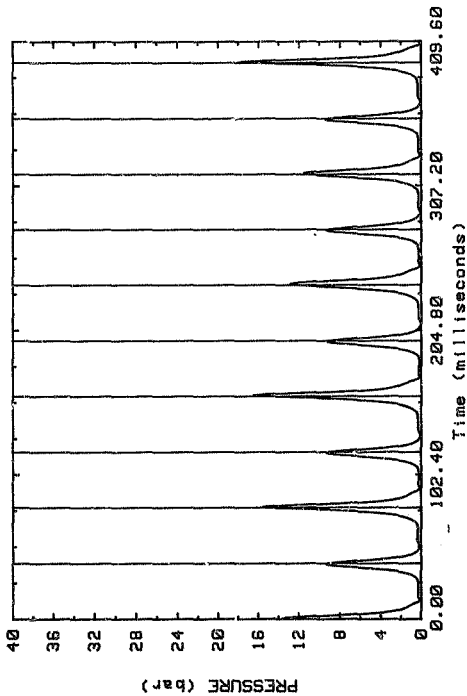


Figure E16 - Pressure trace - mixture cylinder: Test 09108503

CYLINDER 2 : 09108503

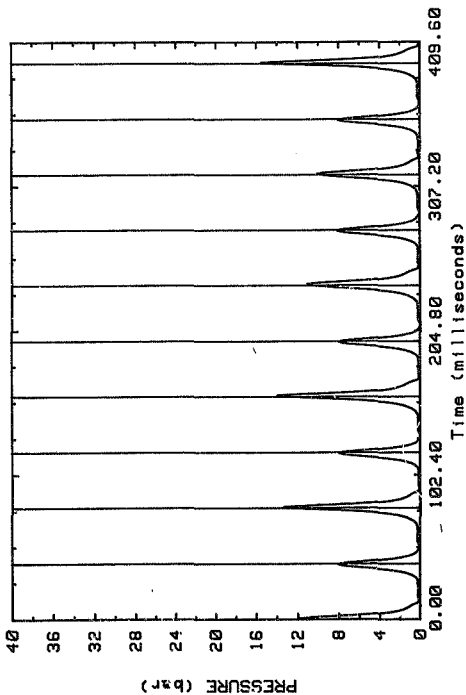


Figure E17 - Pressure trace - air cylinder: Test 09108503

CYLINDERS 1 & 2 : 09108503

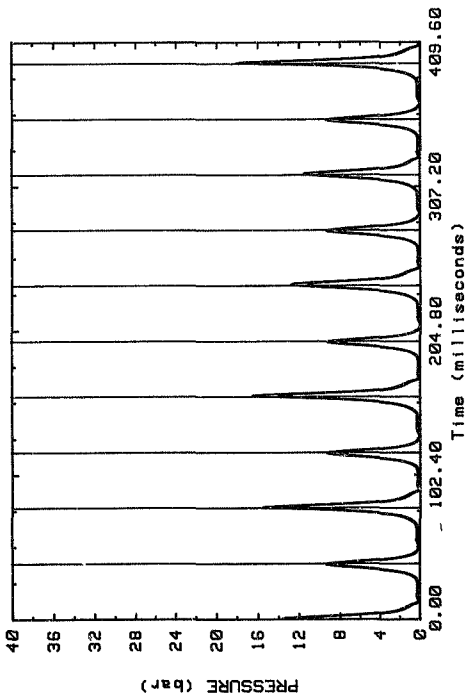


Figure E18 - Pressure trace - both cylinders: Test 09108503

CYLINDER 1 - CYLINDER 2 : 09108503

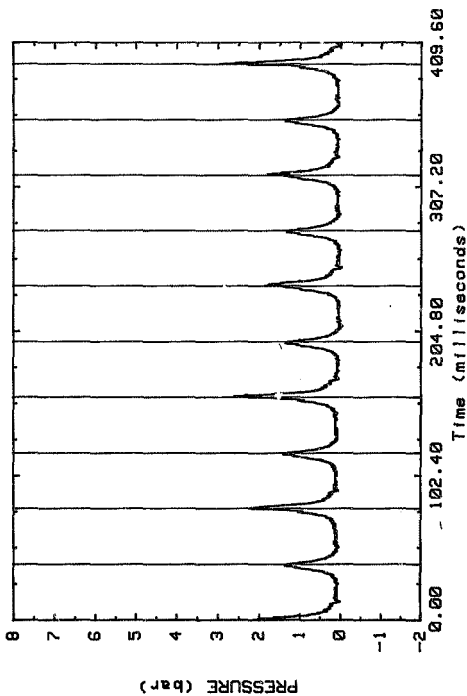


Figure E19 - Pressure trace - differential across cylinders: Test 09108503

SPARK TIMING : 09108503

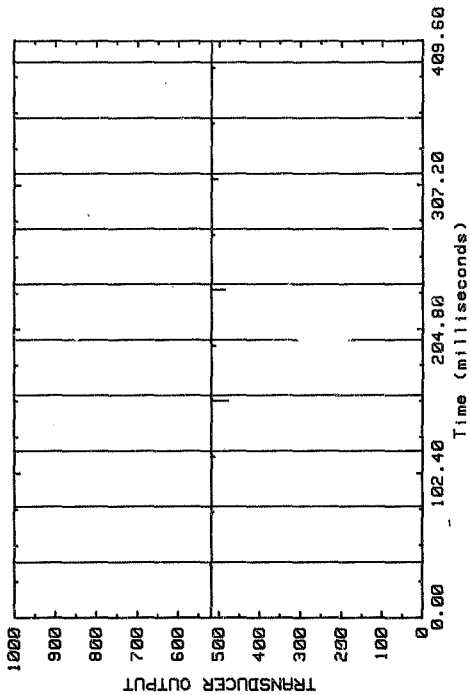


Figure E20 - Spark ignition timing - Test 09108503

CYLINDER 1 : 09108504

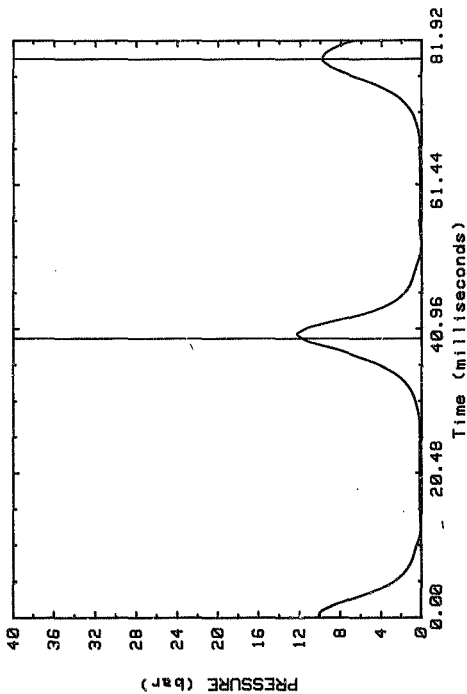


Figure E21 - Pressure trace - mixture cylinder: Test 09108504

CYLINDER 2 : 09108504

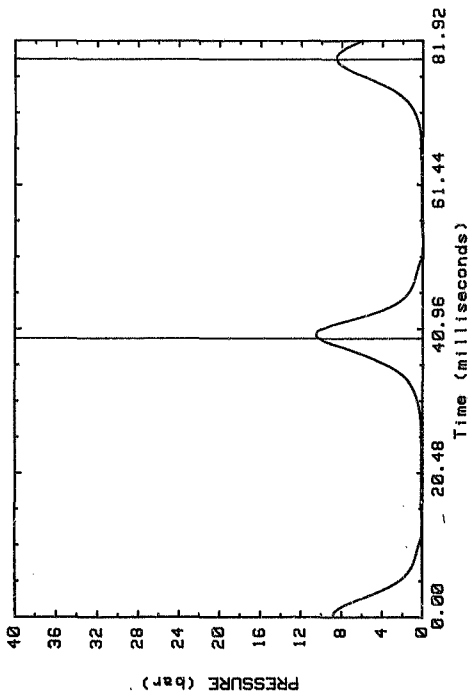


Figure E22 - Pressure trace - air cylinder: Test 09108504

CYLINDERS 1 & 2 : 09108504

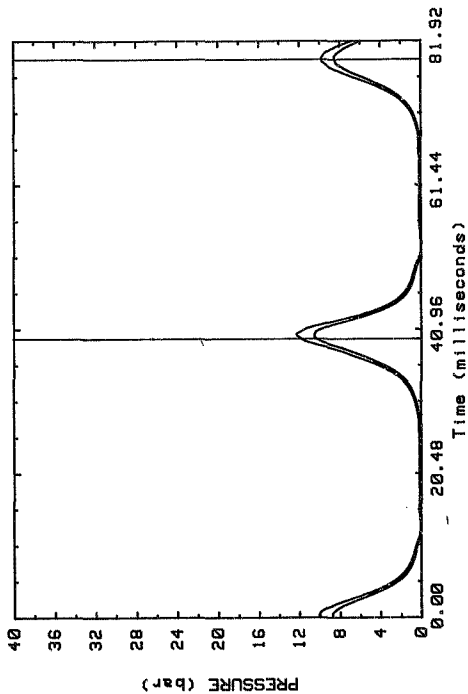


Figure E23 - Pressure trace - both cylinders: Test 09108504

CYLINDER 1 - CYLINDER 2 : 09108504

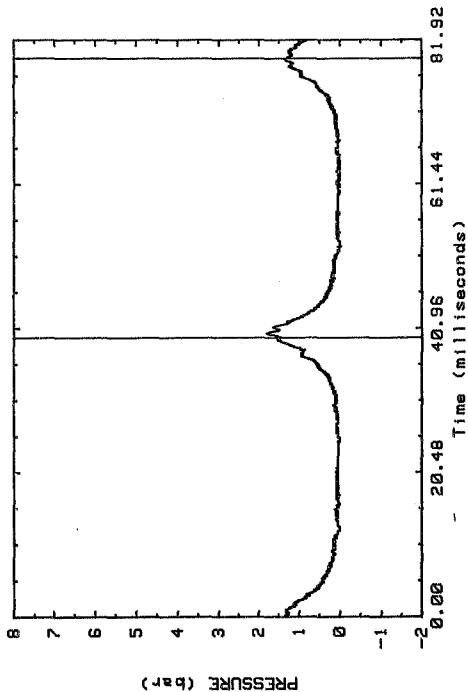


Figure E24 - Pressure trace - differential across cylinders: Test 09108504

SPARK TIMING : 09108504

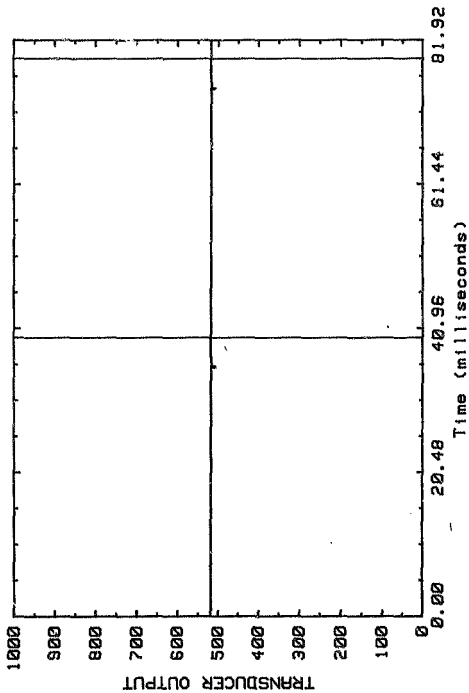


Figure E25 - Spark ignition timing: Test 09108504

For the final test the main fuel jets were rebored to 2,5 mm and the Pierburg fuel flow meters were calibrated and installed (Appendix D, pp D7). Given the analogue output of these meters, it was decided to plot the drop in pressure across the air flow orifice against the required fuel flow for a desired AFR. The engine could then be run at a fixed air-throttle setting, and the fuel needles adjusted to deliver the correct fuel flow for each cylinder for the indicated orifice pressure drop.

For example if the desired AFR = 12,5

$$\text{AFR} = 12,5 = \dot{q}_{\text{air}} / \dot{q}_{\text{fuel}}$$

$$\dot{q}_{\text{air}} = 7,73356 \times 10^{-4} \left[\frac{P[\text{kPa}] \Delta h [\text{mm}]}{T[^\circ\text{K}]} \right]^{1/2}$$

$$\text{Thus } \dot{q}_f = 6,1868 \times 10^{-5} \left[\frac{P[\text{kPa}] \Delta h [\text{mm}]}{T[^\circ\text{K}]} \right]^{1/2} \text{ [kg/s]}$$

Each cylinder has a fitted calibration curve.

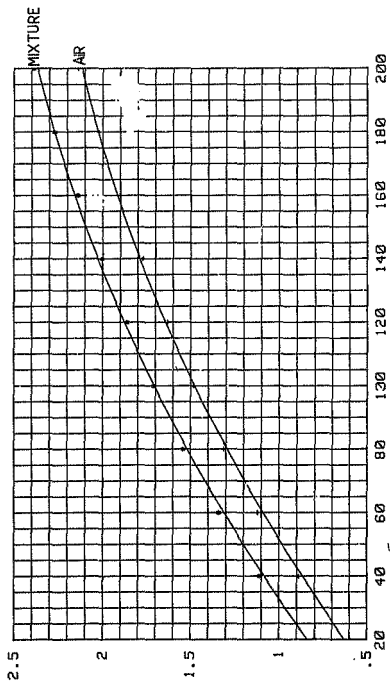
For the mixture cylinder :

$$\dot{q}_f = -0,013997 + .2 \times \dot{q}_{fS} \quad \text{where: } \dot{q}_{fS} = \text{scale reading (1/hr)}$$

$$\dot{q}_f = \text{actual flow (g/s)}$$

$$\text{Substituting: } -0,013997 + .2 \times \dot{q}_{fS} = 6,1868 \times 10^{-5} \left[\frac{P[\text{kPa}] \Delta h [\text{mm}]}{T[^\circ\text{K}]} \right]^{1/2}$$

REQUIRED FUEL FLOW



E30

DELTA P (mmH2O)

Figure E26 - Required fuel flow for AFR = 12.5:1

E31

On the testing day that this graph was used:

$$P_{atm} = 82,64 \text{ KPa}$$

$$T_{in} = 22,4 \text{ }^{\circ}\text{C} = 295,55 \text{ }^{\circ}\text{K}.$$

$$\text{Thus } \dot{q}_{fs} = 1,63574 \times 10^{-1} (\Delta h[\text{mm}])^{3/2} + 0,07 \text{ [1/hr]} \quad \text{[E1]}$$

Similarly, for the air cylinder:

$$\dot{q}_{fs} = 1,59289 \times 10^{-1} (\Delta h[\text{mm}])^{3/2} - 0,1226 \text{ [1/hr]} \quad \text{[E2]}$$

Substituting a range of values for Δh into equations [E1] and [E2] gives the required flow rate to be displayed by the fuel flow meters for each cylinder at an air-fuel ratio of 12,5:1 (Figure E26).

Attempting to use this method proved to be difficult and did not provide the desired engine response. The engine did not run sufficiently stably to attain constant air and fuel flow rates which could be adjusted accurately. The time lag between adjusting the fuel needles and the engine response was long, and the engine did not run at all with the increased AFP's towards 12,5:1. The orifice coefficient calculations were immediately checked.

A calculation was also made to estimate the required air mass flow rate based on the swept volume of the engine at a certain speed. An efficiency of 70% was used (this is reasonable for a two-stroke engine).

Air requirements per engine cycle:

Engine swept volume after the inlet ports have closed:

$$V_{IC} = 760 \times 10^{-6} - \frac{\pi}{4} (0,082)^2 (0,015)(2)$$

$$V_{IC} = 601,57 \times 10^{-6} \text{ m}^3$$

Volumetric efficiency:

$$\begin{aligned} \text{Fresh air required per cycle} &= \eta_v \cdot V_C \\ &= 0.7 \cdot 601.57 \cdot 10^{-6} \\ &= 4.21 \times 10^{-4} \text{ m}^3/\text{cycle} \end{aligned}$$

At engine speed of 1500 rpm = $\frac{1500}{60}$ = 25 cycles/s

$$\begin{aligned} \text{Fresh air requirement} &= 4.21 \times 10^{-4} \times 25 \\ \dot{Q}_{\text{TOT}} &= 10.52 \times 10^{-3} \text{ m}^3/\text{s} \approx 10.52 \times 10^{-3} \text{ kg/s} \end{aligned}$$

The engine running at 1500 rpm, indicated approximately 180 mm drop across the orifice. Thus total air flow

$$\begin{aligned} \dot{Q}_{\text{TOT}} &= 2 \times 7.73356 \times 10^{-4} \left[\frac{82.66 \times 180}{2.9555} \right]^{1/2} \\ \dot{Q}_{\text{TOT}} &= 10.97 \times 10^{-3} \text{ kg/s} \end{aligned}$$

Thus the orifice calculations were cross-checked.

The last test was an attempt to raise the engine speed. Neglecting the previous requirement of balancing the transfer port pressures, each air throttle was varied in turn. The engine stalled whenever the air cylinder throttle was opened. However when the mixture cylinder was opened further than that of the air cylinder throttle, the engine ran to far higher speeds than those previously attained. The speed was in the vicinity of 2500 rpm and resulted in severe vibration due to the engine imbalance. This caused the coupling to overheat and the rubber to collapse. A series of pressure plots was taken at this condition (Figures E27 - E31), and with the ignition timing set at 32° BTDC for MBT. The pressure traces showed no signs of knock, but the peculiar additional change in slope before the exhaust port opened was present.

CYLINDER 1 : 10108501

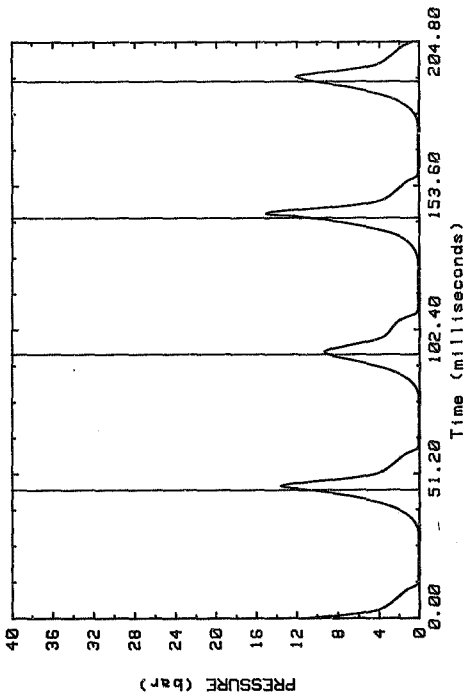


Figure E27 - Pressure trace - mixture cylinder: Test 10108501

CYLINDER 2 : 10108501

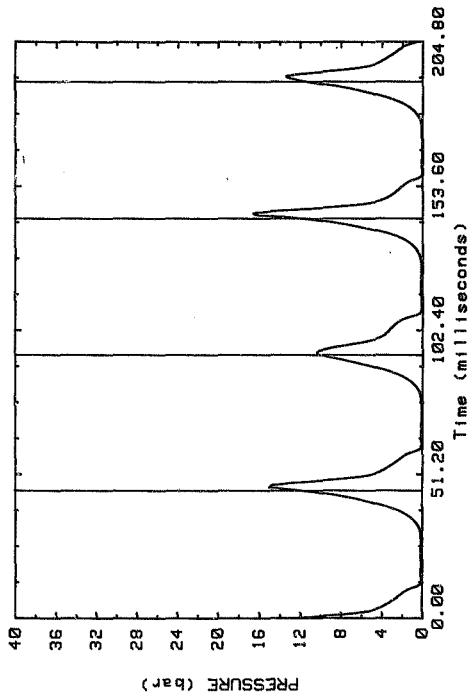


Figure E28 - Pressure trace - air cylinder: Test 10108501

CYLINDERS 1 & 2 : 10108501

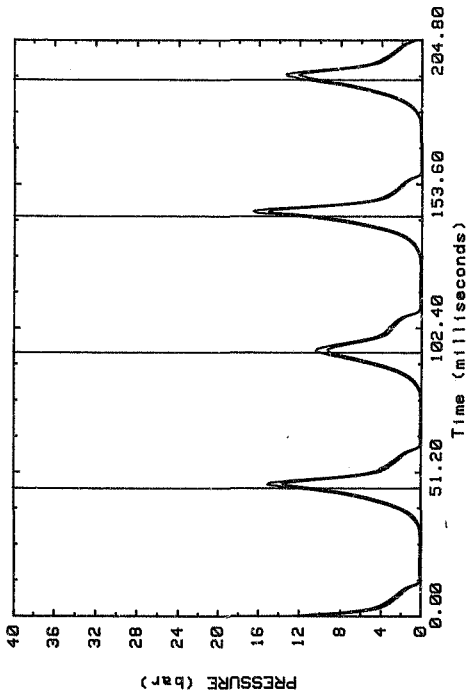


Figure E29 - Pressure trace - both cylinders: Test 10108501

CYLINDER 1 - CYLINDER 2 : 10108501

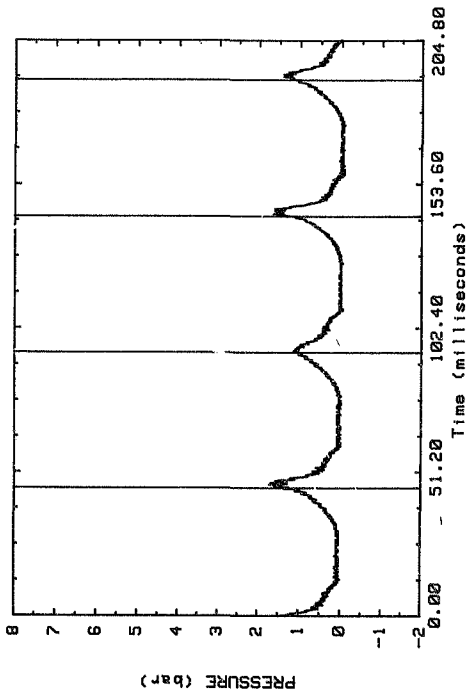


Figure E30 - Pressure trace - differential across cylinders: Test 10108501

SPARK TIMING : 10108501

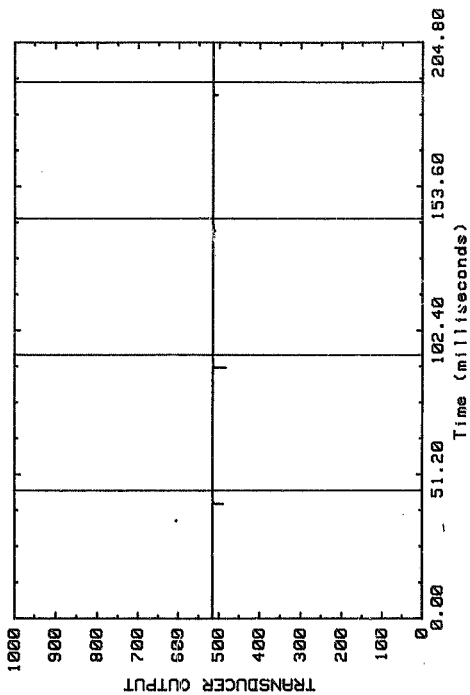


Figure E31 - Spark ignition timing: Test 10108501

APPENDIX F

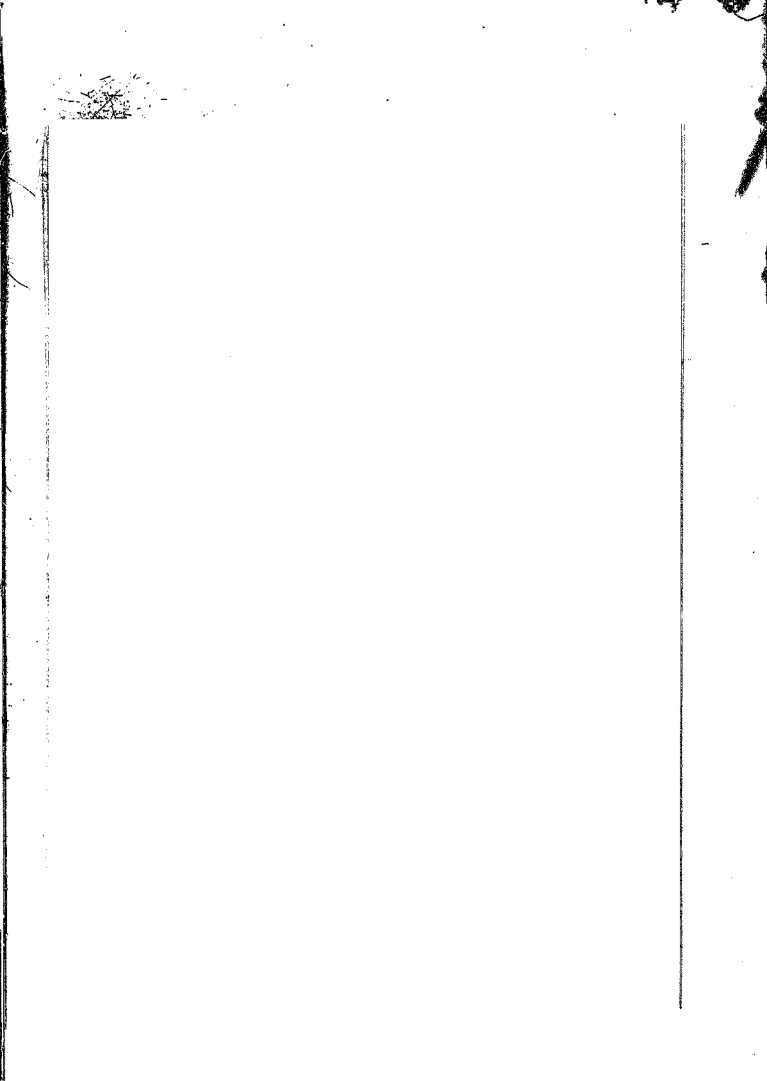
REFERENCES

1. Janicki E (1976) Which auto engine next? *Automotive Engineer* Vol 1, No 7, October/November 1976, 33pp
2. Heywood J B and Tabaczynski R J (1976) Current developments in spark-ignition engines SAE Paper 760606 18pp
3. Uyohara O A, Myers P S, Marsh E E and Cheklich G E (1974) A classification of reciprocating engine combustion systems SAE Paper 741156 presented at the International Stratified Charge Engine Conference, Troy, Michigan October 30 - November 1, 1974, 8pp
4. Dartnell P L (1981) Future engine designs for minimum fuel consumption and exhaust emissions SAE Paper 811385 12pp
5. Germane G J, Wood C G and Hess C C (1983) Lean combustion in spark-ignition internal combustion engines - a review SAE Paper 831694 presented at the Fuels and Lubricants Meeting, San Francisco, California October 31 - November 3, 1983, 20pp
6. Hartley J (1979) Fuel economy and emissions of lean burn engines *Automotive Engineer* Vol 4, No 4, August/September 1979, pp 55-58
7. Date T, Yagi S, Ishizuya A and Fujii I (1974) Why the Honda CVCC Engine meets 1975 emission standards *Automotive Engineering* Vol 82, No 9, pp 50-55 (Based on SAE paper 740605 Research and development of the Honda CVCC engine)
8. Gruden D (1975) A European approach to stratified charge *Automotive Engineering* Vol 83, No 10, pp 56-59

9. Gruden D and Hahn R (1979) Performance, exhaust emissions and fuel consumption of an IC engine operating with lean mixtures Paper C111/79 in IMechE conference publication 1979-9 Fuel economy and emissions of lean burn engines, pp 177-184 Mechanical Engineering Publications Limited, London
10. Stewart R M and Turns S R (1975) The staged combustion compound engine (SCEE): Exhaust emissions and fuel economy potential SAE Paper 750889 presented at the Automobile Engineering meeting, Detroit, Michigan October 13-17, 1975, 22pp
11. Onishi S, Hong Jo S, Do Jo P and Kato S (1984) Multi-layer stratified scavenging (MULS) - a new scavenging method for two-stroke engines SAE Paper 840420 presented at the International Congress and Exposition, Detroit, Michigan February 27 - March 2, 1984, 12pp
12. Yui S and Onishi S (1969) A new concept of stratified charge two stroke engine Yui and Onishi combustion process (YOCP) SAE Paper 690468 presented at the Mid-Year meeting, Chicago, Illinois May 19-23, 1969, 16pp
13. May M G (1979) The high compression lean burn spark ignited 4-stroke engine Paper 97/79 in IMechE conference publication 1979-9 Fuel economy and emissions of lean burn engines, pp 107-116 Mechanical Engineering Publications Limited, London
14. Beale N R and Hodgetts D (1975) The Cranfield-Kushul engine Paper C90/75 accepted for publication by the Institution of Mechanical Engineers on 18th March 1975, London pp 87-95
15. Beale N R and Hodgetts D (1976) Further progress in the development of the Cranfield-Kushul engine SAE Paper 765024 6pp

16. Arques P (1980) Flow and flame propagation in the Kouchoul engine Paper C393/80 IMechE conference publication 1980-9 Stratified charge automotive engines, pp 17-24 Mechanical Engineering Publications Limited, London
17. Tanuma T, Sasaki K, Kaneko T and Kawasaki H (1971) Ignition, combustion, and exhaust emissions in lean mixtures in automotive spark ignition engines SAE Paper 710159 11pp
18. Dale J D and Oppenheim A K (1981) Enhanced ignition for IC engines with premixed gases SAE Paper 810146 presented at the International Congress and Exposition, Cobo Hall, Detroit, Michigan February 23-27, 1981, 20pp
19. Oblander K, Abthoff J and Fricker L (1979) From engine testbench to vehicle - an approach to lean burn by dual ignition Paper (uncoded) in IMechE conference publication 1979-9 Fuel economy and emissions of lean burn engines, pp 19-24 Mechanical Engineering Publications Limited, London
20. Sinnamon J F and Cole D E (1979) The influence of overall equivalence ratio and degree of stratification on the fuel consumption and emissions of a prechamber, stratified charge engine SAE Paper 790438 presented at the Congress and Exposition, Cobo Hall, Detroit, February 26-March 2, 1979, 20pp
21. Yagi S, Fujii I, Ajiki Y and Tsuda T (1980) The antiknock quality in the stratified charge engine with an auxiliary combustion chamber Paper C395/80 IMechE conference publications 1980-9 Stratified charge automotive engines, pp 49-54 Mechanical Engineering Publications Limited, London
22. Yagi S, Fujii I, Nishikawa M and Shirai H (1979) A new combustion system in the stratified charge engine SAE Paper 790439 10pp

23. Kataoka K and Hirako Y (1982) Combustion process in a divided chamber spark ignition engine *Bulletin of the JSME* Paper 210-13, Vol 25, December 1982, 8pp
24. Goulburn J R and Hughes D W (1979) Mixing of vaporized petrol and air in automobile engine inlet systems Paper C96/79 in *IMEchE conference publication 1979-9 Fuel economies and emissions of lean burn engines*, pp 97-106 Mechanical Engineering Publications Limited, London
25. Lucas G G and Brunt M F J (1982) The effect of combustion chamber shape on the rate of combustion in a spark ignition engine SAE Paper 820165 presented at the *International Congress and Exposition, Detroit, Michigan* February 22-26, 1982, 16pp
26. Harrow G A and Clarke P H (1979) Mixture strength control of engine power: Fuel economy and specific emissions from gasoline engines running on fully vaporized fuel/air mixtures Paper C90/79 in *IMEchE conference publications 1979-9 Fuel economy and emissions of lean burn engines*, pp 39-50 Mechanical Engineering Publications Limited, London
27. Sakai Y, Kunii K, Tsutsui S and Nakagawa Y (1974) Combustion characteristics of the torch ignited engine SAE Paper 741167 presented at the *International Stratified Charge Engine Conference, Troy, Michigan* October 30-November 1, 1974, 16pp
28. Hall W L and Sorenson S C (1978) Research on a dual-chamber stratified charge engine SAE Paper 780488 16pp
29. Nel G W and O'Brien T M (1984) Commissioning of a two-stroke two-cylinder lean burn engine Final year research project, *Mechanical Engineering, University of the Witwatersrand*



Author Csatory Peter Robert

Name of thesis Preliminary Testing Of A Two-cylinder Two-stroke Lean Burn Engine Of The Inter-cylinder Connecting Port Type. 1985

PUBLISHER:

University of the Witwatersrand, Johannesburg

©2013

LEGAL NOTICES:

Copyright Notice: All materials on the University of the Witwatersrand, Johannesburg Library website are protected by South African copyright law and may not be distributed, transmitted, displayed, or otherwise published in any format, without the prior written permission of the copyright owner.

Disclaimer and Terms of Use: Provided that you maintain all copyright and other notices contained therein, you may download material (one machine readable copy and one print copy per page) for your personal and/or educational non-commercial use only.

The University of the Witwatersrand, Johannesburg, is not responsible for any errors or omissions and excludes any and all liability for any errors in or omissions from the information on the Library website.